AD-A176 700 MODELING THERMAL ENVIRONMENTS IN LARGE BLAST/THERMAL SIMULATOR (LB/TS) (U) SCIENCE AND ENGINEERING ASSOCIATES INC ALEXANDRIA VA B S CHAMBERS 30 APR 86 1/1

UNCLASSIFIED SEA-63-00-Q-01 DNA-TR-86-192 F/G 18/3 NL

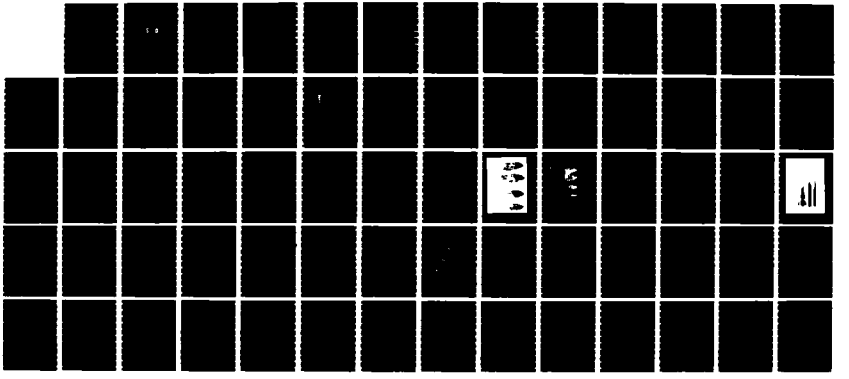

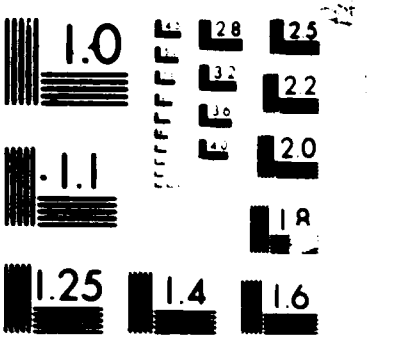
1.0
1.1
1.25
1.4
1.6
2.8
3.2
3.6
2.5
2.2
2.0
1.8

(12)

DNA-TR-86-192

MODELING THERMAL ENVIRONMENTS IN LARGE BLAST/THERMAL SIMULATOR (LB/TS)

Burton S. Chambers III
Science & Engineering Associates, Inc.
P. O. Box 1627
Alexandria, VA 22313

30 April 1986

Technical Report

CONTRACT No. DNA 001-83-C-0158

Approved for public release;
distribution is unlimited.

THIS WORK WAS SPONSORED BY THE DEFENSE NUCLEAR AGENCY
UNDER RDT&E RMSS CODE B345083466 G55AMXGR00009 H2590D

Prepared for
Director
DEFENSE NUCLEAR AGENCY
Washington, DC 20305-1000

Destroy this report when it is no longer needed. Do not return to sender.

PLEASE NOTIFY THE DEFENSE NUCLEAR AGENCY, ATTN: STTI, WASHINGTON, DC 20305-1000, IF YOUR ADDRESS IS INCORRECT, IF YOU WISH IT DELETED FROM THE DISTRIBUTION LIST, OR IF THE ADDRESSEE IS NO LONGER EMPLOYED BY YOUR ORGANIZATION.

DISTRIBUTION LIST UPDATE

This mailer is provided to enable DNA to maintain current distribution lists for reports. We would appreciate your providing the requested information.

☐ Add the individual listed to your distribution list.

☐ Delete the cited organization/individual.

☐ Change of address.

NAME: _____

ORGANIZATION: _____

OLD ADDRESS	CURRENT ADDRESS
_____	_____
_____	_____
_____	_____

TELEPHONE NUMBER: (___) _____

SUBJECT AREA(s) OF INTEREST:

_____	_____
_____	_____
_____	_____

DNA OR OTHER GOVERNMENT CONTRACT NUMBER: _____

CERTIFICATION OF NEED-TO-KNOW BY GOVERNMENT SPONSOR (if other than DNA):

SPONSORING ORGANIZATION: _____

CONTRACTING OFFICER OR REPRESENTATIVE: _____

SIGNATURE: _____

Director
Defense Nuclear Agency
ATTN: STTI
Washington, DC 20305-1000

Director
Defense Nuclear Agency
ATTN: STTI
Washington, DC 20305-1000

UNCLASSIFIED
SECURITY CLASSIFICATION OF THIS PAGE

AD-A176 700

REPORT DOCUMENTATION PAGE

Form Approved
OMB No. 0704-0188
Exp. Date: Jun 30, 1986

1a REPORT SECURITY CLASSIFICATION UNCLASSIFIED	1b RESTRICTIVE MARKINGS
2a SECURITY CLASSIFICATION AUTHORITY N/A since Unclassified	3 DISTRIBUTION/AVAILABILITY OF REPORT Approved for public release; distribution is unlimited.
2b DECLASSIFICATION/DOWNGRADING SCHEDULE N/A since Unclassified	
4 PERFORMING ORGANIZATION REPORT NUMBER(S) SEA 63-00-Q:01	5 MONITORING ORGANIZATION REPORT NUMBER(S) DNA-TR-86-192
6a NAME OF PERFORMING ORGANIZATION Science & Engineering Associates, Inc. 6b OFFICE SYMBOL (If applicable)	7a NAME OF MONITORING ORGANIZATION Director Defense Nuclear Agency
6c ADDRESS (City, State, and ZIP Code) P. O. Box 1627 Alexandria, VA 22313	7b ADDRESS (City, State, and ZIP Code) Washington, DC 20305-1000
8a NAME OF FUNDING/SPONSORING ORGANIZATION 8b OFFICE SYMBOL (If applicable)	9 PROCUREMENT INSTRUMENT IDENTIFICATION NUMBER DNA 001-83-C-0158
8c ADDRESS (City, State, and ZIP Code)	10 SOURCE OF FUNDING NUMBERS PROGRAM ELEMENT NO: 62715H; PROJECT NO: G55AMXG; TASK NO: R; WORK UNIT ACCESSION NO: DH006857

11 TITLE (Include Security Classification)
MODELING THERMAL ENVIRONMENTS IN LARGE BLAST/THERMAL SIMULATOR (LB/TS)

12 PERSONAL AUTHOR(S)
Chambers, Burton S. III

13a TYPE OF REPORT	13b TIME COVERED	14 DATE OF REPORT (Year, Month, Day)	15 PAGE COUNT
Technical	FROM 830317 TO 840228	860430	66

16 SUPPLEMENTARY NOTATION
This work was sponsored by the Defense Nuclear Agency under RDT&E RMSS Code B345083466 G55AMXGR00009 H2590D.

17 COSATI CODES			18 SUBJECT TERMS (Continue on reverse if necessary and identify by block number)	
FIELD	GROUP	SUB-GROUP		
14	2		Nuclear Weapons Effects	Blast/Thermal Simulator
19	4		Thermal Radiation Simulators	Scaling TRS Data
			Modeling Simulated Environments	TRS Data

19 ABSTRACT (Continue on reverse if necessary and identify by block number)

The work reported herein was conducted in support of the use of aluminum-liquid oxygen (LOX) thermal radiation simulators (TRS) in the planned large blast/thermal simulator (LB/TS). The type of TRS is the so-called flame or torch TRS.

The tasks performed during this work consisted of the following activities:
(1) the ~~DNA~~ TRS predictor models were extended to account for different burn rates,
(2) conditions unique to the LB/TS were considered from a modeling viewpoint,
(3) four camera systems were used to characterize the spectral and temperature variations of a ~~DNA~~ four nozzle TRS ~~at~~ Kirtland AFB, NM,
(4) calorimeter baffles were designed, constructed, and used to obtain source-resolved irradiance data.

Relationships to scale TRS output to fuel flow rate were hypothesized and compared to

20 DISTRIBUTION/AVAILABILITY OF ABSTRACT	21 ABSTRACT SECURITY CLASSIFICATION
☐ UNCLASSIFIED/UNLIMITED ☒ SAME AS RPT ☐ DTIC USERS	UNCLASSIFIED
22a NAME OF RESPONSIBLE INDIVIDUAL Betty L. Fox	22b TELEPHONE (Include Area Code) (202)325-7042
	22c OFFICE SYMBOL DNA/STTI

DD FORM 1473, 84 MAR 83 APR edition may be used until exhausted
All other editions are obsolete

SECURITY CLASSIFICATION OF THIS PAGE
UNCLASSIFIED

19. ABSTRACT (Continued).

available data. The results are encouraging but inconclusive. With the existence of source-resolved irradiance data, an improvement was made to the TRS predictor models; this improvement has applicability to TRS use in predicting free-field environments.

The photographic and spectral measurement made in the visible were useful to understanding the TRS flame structure. The baffled calorimeter experiments yielded data directly usable to improve models.

SUMMARY

The work reported herein was conducted in support of the use of aluminum-liquid oxygen (LOX) thermal radiation simulators (TRS) in the planned large blast/thermal simulator (LB/TS). This facility is being considered for development by Defense Nuclear Agency (DNA). The type of TRS is the so-called flame or torch TRS, which consists of a set of nozzles each burning aluminum powder in sprayed liquid oxygen (LOX). Unless otherwise noted, use of the acronym, "TRS", means the Al-LOX flame TRS.

The tasks performed during this work consisted of the following activities: (1) the DNA TRS predictor models were extended to account for different burn rates, (2) conditions unique to the LB/TS were considered from a modeling viewpoint, (3) four camera systems were used to characterize the spectral and temperature variations of a DNA four nozzle TRS at Kirtland AFB, NM for three TRS burns, (4) calorimeter baffles were designed, constructed, and used to obtain source-resolved irradiance data.

Relationships to scale TRS output to fuel flow rate were hypothesized and compared to available data. The results are encouraging but inconclusive; the trends that have been inferred will warrant further inspection when more data become available. In addition, with the existence of source-resolved irradiance data, it was possible to make a basic improvement to the TRS predictor models. This improvement also has applicability to TRS use in predicting free-field environments.

The photographic and spectral measurement made in the visible spectrum were useful in better understanding the TRS source. An attempt, however, should also be made to model these photographic and spectral measurement results. Further, measurements in the infrared would help determine the nature of the flame's radiance; these could be compared with the optical data.

The baffled calorimeter experiments that were performed are new to TRS; these yielded useful data. It is recommended that these new baffled calorimeter data be reacquired on a dedicated set of TRS burns and a larger number of calorimeters be used.

There is currently no way to assess calorimeter response just prior to a shot. A readiness condition is tested by briefly exposing each calorimeter to the flame of a portable propane torch. Response is noted but not quantized. To assure a common base to the data, and that certain biases have not been introduced, spot checks should be developed for the LB/TS and also the field.

PREFACE

The work reported herein was performed by Science and Engineering Associates, Inc. (SEA) for Defense Nuclear Agency (DNA) under contract No. DNA 001-83-C-0158 during the period 17 March 1983 - 28 February 1984. The program manager for this work (and the SEA principal investigator) was Mr. Burton S. Chambers III. A subcontractor, Information Sciences Incorporated (ISI), and its subcontractor, Sandia National Laboratories in Albuquerque (SNL/A), supported SEA on this effort. The ISI principal investigator was Dr. Walter Dudziak. Dr. Harold Linnerud led the SEA fielding task.

This work was conducted for the Shock Physics Test Division (SPTD) at Headquarters, DNA, in support of the Large Blast/Thermal Simulator (LB/TS) program. It was coordinated with the Ballistics Research Laboratory (BRL) at Aberdeen Proving Ground, Maryland. Testing support was provided by Field Command DNA (FCDNA) and their contractor, Bendix Corporation, at the TRS site.

LTC Robert Flory, United States Army (USA), was the DNA Contract Technical Manager (CTM). Mr. George Teel and Dr. Andy Mark were the points of contact at BRL. Lt. Col R. Bousek and LCDR William Taylor were the points of contact at FCDNA. Mr. Ed Welsh represented Bendix at the TRS site.

The author thanks LTC Flory, Mr. Teel, and Dr. Mark for their useful guidance and suggestions during the technical effort and Lt. Col. Bousek, LCDR Taylor, and Mr. Welsh for their support during the TRS testing phase. The continuing interest of Mr. Tom Kennedy, SPTD, is also most appreciated.

Finally, the author would like to express his appreciation for the fruitful technical discussions with Dr. Dudziak, president of ISI. The wealth of data provided by him and his team should prove useful to modeling TRS environments.

CONVERSION TABLE

Conversion factors for U.S. Customary to metric (SI) units of measurement.

MULTIPLY →	BY →	TO GET
TO GET ←	BY ←	DIVIDE

angstrom	1.000 000 X E -10	meters (m)
atmosphere (normal)	1.013 25 X E +2	kilo pascal (kPa)
bar	1.000 000 X E +2	kilo pascal (kPa)
barn	1.000 000 X E -28	meter^2 (m^2)
British thermal unit (thermochemical)	1.054 350 X E +3	joule (J)
calorie (thermochemical)	4.184 000	joule (J)
cal (thermochemical)/cm^2	4.184 000 X E -2	mega joule/m^2 (MJ/m^2)
curie	3.700 000 X E +1	giga becquerel (GBq)*
degree (angle)	1.745 329 X E -2	radian (rad)
degree Fahrenheit	$t_K=(t°f+459.67)/1.8$	degree kelvin (K)
electron volt	1.602 19 X E -19	joule (J)
erg	1.000 000 X E -7	joule (J)
erg/second	1.000 000 X E -7	watt (W)
foot	3.048 000 X E -1	meter (m)
foot-pound-force	1.355 818	joule (J)
gallon (U.S. liquid)	3.785 412 X E -3	meter^3 (m^3)
inch	2.540 000 X E -2	meter (m)
jerk	1.000 000 X E +9	joule (J)
joule/kilogram (J/kg) (radiation dose absorbed)	1.000 000	Gray (Gy)**
kilotons	4.183	terajoules
kip (1000 lbf)	4.448 222 X E +3	newton (N)
kip/inch^2 (ksi)	6.894 757 X E +3	kilo pascal (kPa)
ktap	1.000 000 X E +2	newton-second/m^2 ($N-s/m^2$)
micron	1.000 000 X E -6	meter (m)
mil	2.540 000 X E -5	meter (m)
mile (international)	1.609 344 X E +3	meter (m)
ounce	2.834 952 X E -2	kilogram (kg)
pound-force (lbf avoirdupois)	4.448 222	newton (N)
pound-force inch	1.129 848 X E -1	newton-meter (N·m)
pound-force/inch	1.751 268 X E +2	newton/meter (N/m)
pound-force/foot^2	4.788 026 X E -2	kilo pascal (kPa)
pound-force/inch^2 (psi)	6.894 757	kilo pascal (kPa)
pound-mass (lbm avoirdupois)	4.535 924 X E -1	kilogram (kg)
pound-mass-foot^2 (moment of inertia)	4.214 011 X E -2	kilogram-meter^2 ($kg·m^2$)
pound-mass/foot^3	1.601 846 X E +1	kilogram/meter^3 (kg/m^3)
rad (radiation dose absorbed)	1.000 000 X E -2	Gray (Gy)**
roentgen	2.579 760 X E -4	coulomb/kilogram (C/kg)
shake	1.000 000 X E -8	second (s)
slug	1.459 390 X E +1	kilogram (kg)
torr (mm Hg, 0°C)	1.333 22 X E -1	kilo pascal (kPa)

* The becquerel (Bq) is the SI unit of radioactivity; 1 Bq = 1 event/s.
**The Gray (Gy) is the SI unit of absorbed radiation.

TABLE OF CONTENTS

LIST OF ILLUSTRATIONS

LIST OF TABLES

SECTION 1

INTRODUCTION

The United States Army has nuclear weapon effects (NWE) requirements that must be met in order for the Army to effectively assure its systems survivability in the undesirable event of a limited nuclear war. In order to assess system survivability, the Army has identified a need for a large shock tube to deliver realistic air blast loads on fairly large drag-sensitive targets. Since it is also recognized that synergistic air blast and thermal effects can be important to these system survivability assessments (Reference 1), thermal loads also need to be delivered within the shock tube.

Therefore, the Army is proceeding with a program that may lead to a decision to develop, design, construct and calibrate a large blast simulator with an internal thermal simulator. In support of the Army requirements, Defense Nuclear Agency (DNA) is participating in this Large Blast/Thermal Simulator (LB/TS) program by providing research and development support in critical technology areas.

This report presents the results of one such effort where DNA is providing support to the LB/TS program. This effort was conducted to extend existing tools for calculating the irradiance at locations in front of thermal simulators planned to be placed in the LB/TS.

1.1 THERMAL RADIATION SIMULATOR (TRS).

One of the most important differences between a nuclear explosion (NE) and a chemical high explosive (HE) is the relatively large amount of energy released during the nuclear explosion in the form of thermal radiation. Synergistic effects, resulting from the combination of air blast and thermal loads, have been seen in the nuclear case; they have been known to exist for many years. Unfortunately, these effects have been difficult to obtain in the field primarily due to lack of large scale thermal simulation devices that produce significant radiative output.

Therefore, DNA has been investigating ways to improve its thermal simulation capability. One such approach was developed by Science Applications, Inc. (SAI) and resulted in a large scale thermal radiation simulator (TRS), the Al-LOX system. A number of these simulators have been fielded on the last three DNA HE events: MILL RACE, DIRECT COURSE, and MINOR SCALE. They are planned to be used in the LB/TS in order to investigate synergistic thermal air blast effects.

The type of TRS being considered will consist of a set of nozzles aligned in a row. Each nozzle will work like current TRS nozzles in that it will spray aluminum powder, fluidized in a nitrogen bed, rapidly upward into the air while liquid oxygen is being ejected into this two phase flow. The mixture will be ignited and will produce an intense flame that can burn until the constituents are throttled or exhausted. Each current TRS flame typically reaches a height of four to eight meters. The height of the TRS in the LB/TS will be determined by how it is operated and details of the flow within the LB/TS.

For use in the LB/TS, the consumed products of combustion are

planned to be vented through the roof prior to air blast arrival. A series of gas driven ejector nozzles is expected to be used to assist in the removal of TRS debris. Because the thermal radiation produced is small when compared with a nuclear burst, it is necessary to place the flames relatively close to any target that is to be irradiated.

1.2 MODELING OF TRS RADIATED ENVIRONMENT WITHIN LB/TS.

The motivation for modeling TRS radiated environments for LB/TS conditions as soon as possible is to allow planning to occur. The TRS models developed for DNA thus far do a reasonably good job in replicating the data taken in the field. The model parameters are determined by calibrating to the field data. The calibrated models have value in that their existence allows reliable interpolations to be made for planning field experiments.

Current TRS models, however, need to be extended. Account of wall reflections that will naturally exist in the LB/TS must be made. The physical models also have to be adjusted for different flow rates.

The current planning for LB/TS assumes a reliable thermal estimator will be available to help in its design. This effort was therefore directed toward extending the current DNA models to LB/TS conditions with plans to perform calculations that the LB/TS community could use for preliminary planning. Nevertheless, it is expected that these models will be further refined and calibrated as additional experimental data become available.

1.3 BRIEF HISTORY OF MODEL DEVELOPMENT.

When the first TRS modeling efforts were started for DNA, the intention was to provide empirical fits to the data as it was being collected. Nevertheless, the modeler chose physically plausible models and potentially meaningful adjustable parameters in the hope that the model parameters would someday be correlatable to actual physical data. As it turned out years later, correlations were established and a general calibration to the TRS source, with a 5 kilogram per second flow rate of aluminum, produced results in reasonable agreement with the database. Furthermore, model parameters that would represent visual flame dimensions agreed approximately with the photographed flame shape.

This success prompted the limited field of view experiment in an attempt to improve the understanding of height dependency of some of the other model parameters. The results have been encouraging and analysis has led to an improved representation of the flame. Additional details about the model can be found in Reference 2.

1.4 EXPERIMENTS NEEDED TO MODEL THERMAL IN LB/TS

The original point source TRS model has been improved through several iterations to reach the current bulging inverted cone model (Reference 2. Model improvements have generally been supported by the limited data acquired on TRS test firings. Even with these improvements, there are still significant differences between predicted and measured irradiance levels at some positions. These differences can have several sources including both model error and measurement error. These are related because the model has been developed and validated with the aid of the existing measurement data

base. The data base is limited and therefore errors within it will significantly impact model performance.

It is however, just such a detailed model which must be developed for the LB/TS. To date, the TRS has chiefly been used in field experiments. In that case, the primary reflective surface is the ground. In the LB/TS, the TRS will be largely confined and the walls of the structure may influence the thermal load delivered to a target. Additionally, a detailed knowledge of TRS source characteristics will assist in the selection of LB/TS construction materials and also perhaps in physical design. To support the development and validation of a detailed model, the TRS must be characterized with a higher degree of spatial and spectral resolution.

Such an experimental program was conducted with the objective to significantly increase the existing database on TRS source characteristics. This objective was partially achieved by using radiometrically calibrated scientific photography and also by using calorimeters with restricted fields-of-view.

Scientific photography was used to generate detailed two-dimensional mappings of the TRS radiating source. The films to be used were calibrated to provide a measure of film response (measured density) to incident energy (exposure). The curve generated (the H&D curve) was then used to convert film density measurements to source radiance levels and detailed two-dimensional source characterizations resulted. Additionally, by using a diffractive medium (prism) in the optical path, data were simultaneously acquired on radiance levels and spectral content along selected traverses of the TRS source. A field-of-view tilted across four TRS flames acquired data on both vertical radiance levels and on spectral content for effective "temperature" correlations.

Such detailed mapping was supported by using calorimeters baffled to limit their field-of-view. Such measurements provide information on irradiance levels from selected portions of the TRS flame (e.g., from horizontal slices across the flame). Ideally, the film and calorimeter measurements can be correlated to provide increased confidence in both the model and the measurement techniques.

SECTION 2

USING TRS IN LB/TS AND AVAILABLE DATA

This section discusses the models that need to be modified in order to be used for LB/TS. The LB/TS conditions that differ from the field when operating the TRS are then presented. These are followed by an overview of data used, but not generated, during this effort. Finally, earlier estimates of energy incident on a shock tube wall are shown to illustrate the need for that type of data.

2.1 INVERTED CONE TRS MODEL.

The model, which existed at the beginning of this effort, numerically simulates each flame and its shadowing effect on any others. It then calculates the peak irradiance incident upon a surface that is facing the flames and is oriented in some specified direction. The irradiance is the amount of thermal energy (heat and light) crossing this surface per unit area and time. Each flame is represented by a cone with apex at the nozzle (referred to here as an inverted cone). Account is made of a height dependence of the flame's radiated power per each unit length. The approach is to use a linearly changing power per unit length up to some height approximating the flame.

In this model, each flame is treated as a linear array of point sources except when a flame is partially obscured. The number of points depends on the distance between the flame and field point so as to maintain acceptable accuracy. The closer the detector (the receiving surface) is to the flame, the larger the number of points. This approach has been verified and accurately represents the output from a line source (Reference 2).

When a flame is shadowed, it is treated as an array of stacked discs, each with radius corresponding to the flame width at that height. The contribution to the flux from each shadowed disk is adjusted by the amount of shadowing and an appropriate change in view angle. The radiating portion of the flame is approximated as a diffuse source for shadowed flames.

Capping each flame with an opaque cylinder approximates the influence from smoke generated by the flames and completes the model.

A more detailed discussion of the inverted cone and earlier TRS predictor models can be found in Reference 3. In order to use the model, its parameters must be determined by a process called calibration; Reference 3 contains a discussion of this process. Much of the data used to calibrate the 5 kilogram per second source model is in References 2 and 3.

2.2 LB/TS CONDITIONS.

Conditions within the LB/TS will be different than prior use of the TRS in the field and can be expected to influence the generated environment. The conditions are: (1) existence of walls, (2) existence of vents, and (3) air curtains near the flames. Any influence targets may have on TRS performance was not evaluated in this effort.

The existence of walls will cause some of the energy that would

otherwise be radiated away from the target to be scattered back and will tend to enhance the environment. The existence of vents will reduce somewhat this enhancement. Both the walls and vents will affect the flow, which is into the flames, and therefore may affect TRS performance. Figure 1 shows a simplified view of one LB/TS concept; it shows the relationship between source, wall, and target (detector).

A concept to help vent the residue from TRS burning is to install air curtains to help direct the combustion products out the top of the tube. These are not shown in Figure 1, but would flow from the bottom of the tube, along the flame, and through the vent. The influence of the forced flow, originating at the air curtains, on the entrained flow along the turbulent flame edge is expected to change the radiance from the TRS. The popular view is that the air curtain will modestly enhance TRS radiance.

The LB/TS will probably use a different TRS than that currently being used in the field. Since changes to the TRS or its operating conditions can also affect its performance, some of these differences must be considered.

2.3 TRS DATABASES.

Numerous databases have been developed from the experimental measurements recorded during the past years of TRS firings. Most of the data exist for the TRS burning nominally 5 kilograms of aluminum per second. Most of the knowledge gained about TRS variability resulted from the collection and analysis of this database (Reference 3).

Each of these databases represents some subset of available TRS data; each can be used to calibrate the model for some conditions to be simulated. When successful in achieving a replication of the chosen experimental data, a database may provide an indication of the overall variability to be expected during actual experiments. This point is important because the TRS operation although becoming more reliable is certainly still quite variable. Reference 3 presents more information on the 5 kilogram per second database.

There also exist some data for another aluminum flow rate: the one kilogram per second data generated at BRL with a smaller TRS developed a few years ago. This smaller TRS is described in Reference 4. The data in that reference were available for use during this program from References 5 and 6; Reference 6 includes data extending the range out past one meter to almost three meters. The data used from these references is presented in the next subsection.

2.4 ONE KG/SEC TRS DATA BASE

The database chosen for the calibration was the two second burn set: shots 1, 5A, and 10 from Reference 5 and data provided by Teel (Reference 6). (Note that this burn time is actually the fuel flow time). Fluence at five seconds was used to model the data; however, the flux and fluence are not simply related by this burn time. In fact, the average of the ratio of fluence divided by peak flux for the data in Reference 5 is about 2.8 on average, not two.

When comparing data from the TRS at FCDNA and that from BRL, the reader must bear in mind that the two organizations use different definitions

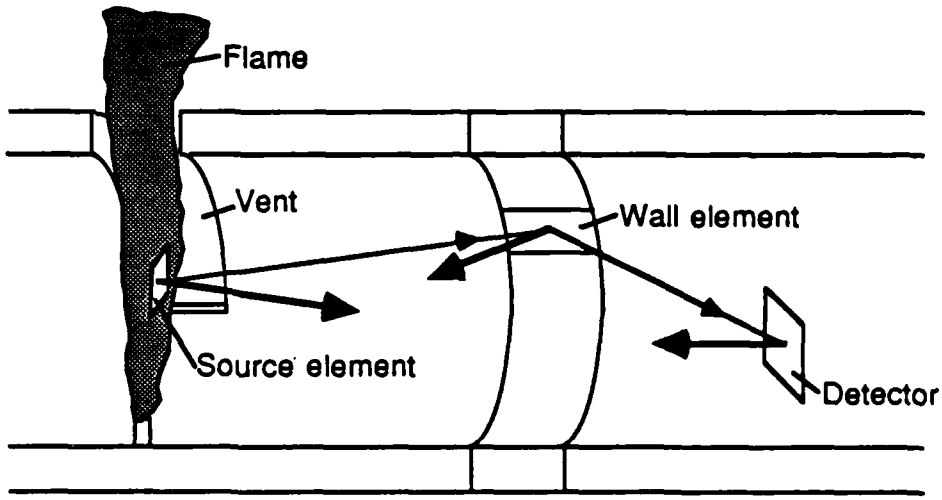

Figure 1. Scattered radiation in LB/TS.

for burn time. A two second burn time at FCDNA means that the fluence divided by peak flux is intended to equal two; this is imprecise but defines their burn time. At BRL, on the other hand, a two second burn means that aluminum is being pumped into the system for two seconds. Since the aluminum will be dispersed while flowing through the fuel lines and since it takes some time to burn while aloft, the ratio of fluence to peak flux will generally be larger than the BRL burn time. We have accounted for these differences when scaling the two data sets.

Inspection of Reference 4 reveals that the flame for the 1 kilogram per second BRL TRS is asymmetric; this is consistent with data sent by Teel (Reference 7). No attempt was made to model these asymmetries, but instead concentrated on the data nominally in front of the nozzle axis.

Table 1 presents the database generated during this effort based on the BRL measurements just discussed. Please note that the table shows fluence rather than peak flux; the latter is typically what is modeled, therefore care must be taken when comparing this table with other databases. Fluence was compared rather than flux because at the time the fluence data were available in the range from 25 to 265 cm., whereas the peak flux was only available in the interval from 25 to 75 cm.

2.5 TRS ENVIRONMENT AT THE LB/TS WALL.

Once sufficient data are available that describe the TRS to be used in the LB/TS, calculations similar to those generated prior to this effort (Figure 2) can be performed to enable LB/TS planners to evaluate such questions as: what are the stresses on the tube wall from nonuniform thermal loading from the TRS. The particular calculations shown here were based on unvalidated scaling relationships. Further, the TRS was assumed to consist of three nozzles: the outer two each burning 1 kilogram of aluminum per second; and the inner one burning 2 kilograms per second. These results are provided only as an illustration of why it is perhaps important to model the TRS before the LB/TS is built.

Table 1. BRL fluence database.

Range cm.	Height cm.	Fluence col/sqcm	Shot	cal ID
25	109	239.0	1	1
25	61	216.0	1	2
50	109	113.0	1	3
50	61	90.0	1	4
90	109	60.0	1	5
90	61	52.0	1	6
25	109	210.0	5A	1
25	61	211.0	5A	2
50	109	95.0	5A	3
50	61	99.0	5A	4
90	109	54.0	5A	5
90	61	44.0	5A	6
30	109	155.0	10	1
30	61	155.0	10	2
40	109	13.0	10	3
40	61	16.0	10	4
70	109	70.0	10	5
70	61	56.0	10	6
90	109	54.8	?	1
90	61	45.9	?	2
120	109	31.3	?	3
120	61	24.4	?	4
150	109	23.5	?	5
150	61	18.8	?	6
185	109	17.6	?	7
185	61	13.9	?	8
200	109	16.0	?	9
200	61	13.9	?	10
230	109	13.5	?	11
230	61	12.0	?	12
265	109	11.5	?	13
265	61	9.8	?	14

All calorimeters are directly facing the nozzle's nominal centerline.
First section presents data from Reference 5.
Second section are averages from data in Reference 6.

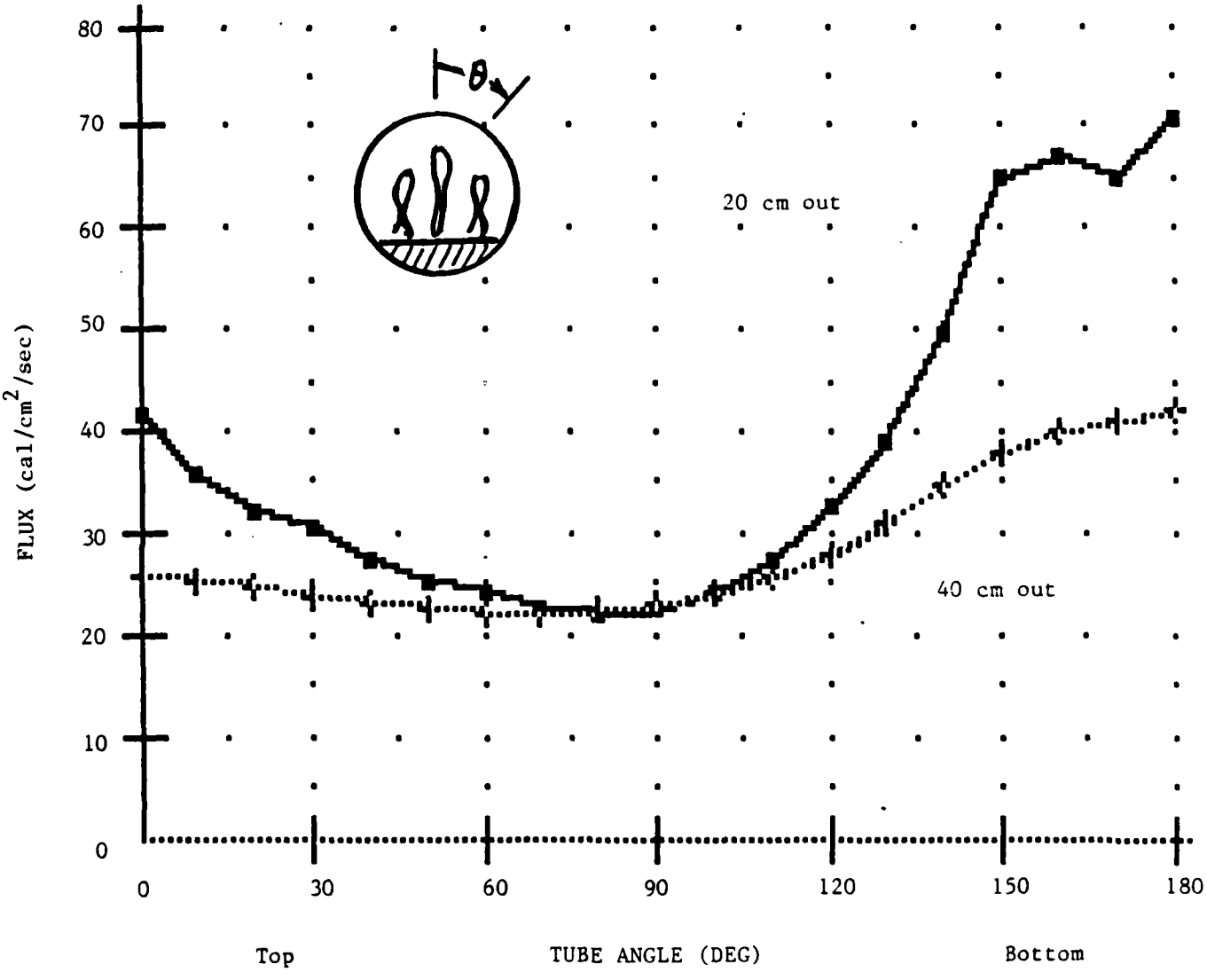

Figure 2. Flux incident on inside wall.

SECTION 3

TRS MODELING EXTENSIONS

The objective of the modeling work on this effort was to extend the DNA TRS thermal predictor models to LB/TS conditions. The result of the effort was: (1) to improve the power per unit height relationship; (2) to account for potentially different fuel flow rates; and (3) to consider how to include the capability for treating wall reflections (with postulated vents). These are briefly discussed here.

First, the power per unit height relationship in the model was improved as a direct result of interpretation of data obtained on this effort and discussed in Section 5. Second, comparison of BRL one kilogram per second TRS data and models of the 5 kilogram per second source led to the conclusion that the power scaled to within 14 percent of what had been expected, and the modeled flame height scaled between two scaling hypotheses (12 feet instead of 8.4 feet and 14.4 feet). Third, the wall reflection approach was formulated, but not implemented due to a required emphasis on the experimental tasks.

The only data available that could be used to determine how the model parameters might scale were the BRL data taken earlier (References 4 and 5) and data being generated during the same time frame as this technical effort (Reference 6). These data were generated with a torch typically flowing aluminum at the rate of one kilogram per second, or about 20 percent of the usual rate for the 5 kilogram per second burner at the FCDNA TRS site.

The net result of the study was that a way of scaling the 5 kilogram per second data was found that produced good agreement with the 1 kilogram per second source. However, it is clear that multiple solutions are possible and it, therefore, can not be said that the scaling relationship is known. Additional measurements will be required, possibly with spatial resolution type gauges similar to what was used in this effort.

3.1 SCALING FLAME SHAPE.

Although the results are inconclusive, it can be said that no serious error seems to be introduced if the shape of the flame's profile is taken to be invariant when scaled by two model parameters: flame height and flame diameter. (These parameters are also changed and are determined by a calibration to the data). Note that it is possible that availability of height resolved irradiance data could lead to adjusting the shape.

The determination of all the model parameters was made by a calibration to the fluence data in References 5 and 6, which were later published in Reference 4. The set of model parameters thus determined are compared with those for the 5 kilogram per second source adjusting to account for the fact that fluence data were being used. The comparison allowed the tentative evaluation of scaling hypotheses. The new parameters were used to generate calculations with the model and these results were compared with the original data.

The agreement was improved by modifying the older model as found in the original version of FC-TEE (Reference 8) to account for the fact that the flame profile is not really an inverted cone but bulges out nearer to the

ground as seen in Figure 3. This improvement has been included in FC-TEE II (Reference 9).

Making the aforementioned adjustments in model parameters and model improvements, a calibration of the model was produced. Then the model was exercised for conditions that included the database and the two were compared. Figures, 4 and 5, show the result which appears quite good. Because no flux data were available past one meter in range (and funds were limited) no calibration to peak flux or subsequent comparison was made.

Although sufficient data do not exist to validate what has been learned about scaling the TRS models to different operating conditions, this effort showed promising results.

3.2 EXTENDING MODEL TO INCLUDE WALL REFLECTIONS.

The LB/TS will probably have diffuse walls. If this is the case then it will be computationally efficient to first precompute and then model the flux incident at each location on the wall, since the position of the detector will not affect this (assuming small detectors). This will be true whether or not the flame structure is static.

However, if a specular component exists it may be better to model at least the specular part for any detector since each source element (see Figure 1 shown earlier) will have a different image for each detector. This image will appear to the detector as a ring beyond the wall.

Some experimental work has been done that indicates that the contribution from the wall with vents will be small (Reference 10). Since the flame source has not been modeled, it is difficult to determine with any confidence whether these preliminary experimental results would be expected based on theoretical arguments. Calculating the importance of wall reflections will not be difficult once the flame source and reflecting nature of the wall are known. The primary issues will be how to efficiently compute the environment and that will depend on what the conditions (e.g., wall reflectivity and flame structure) are.

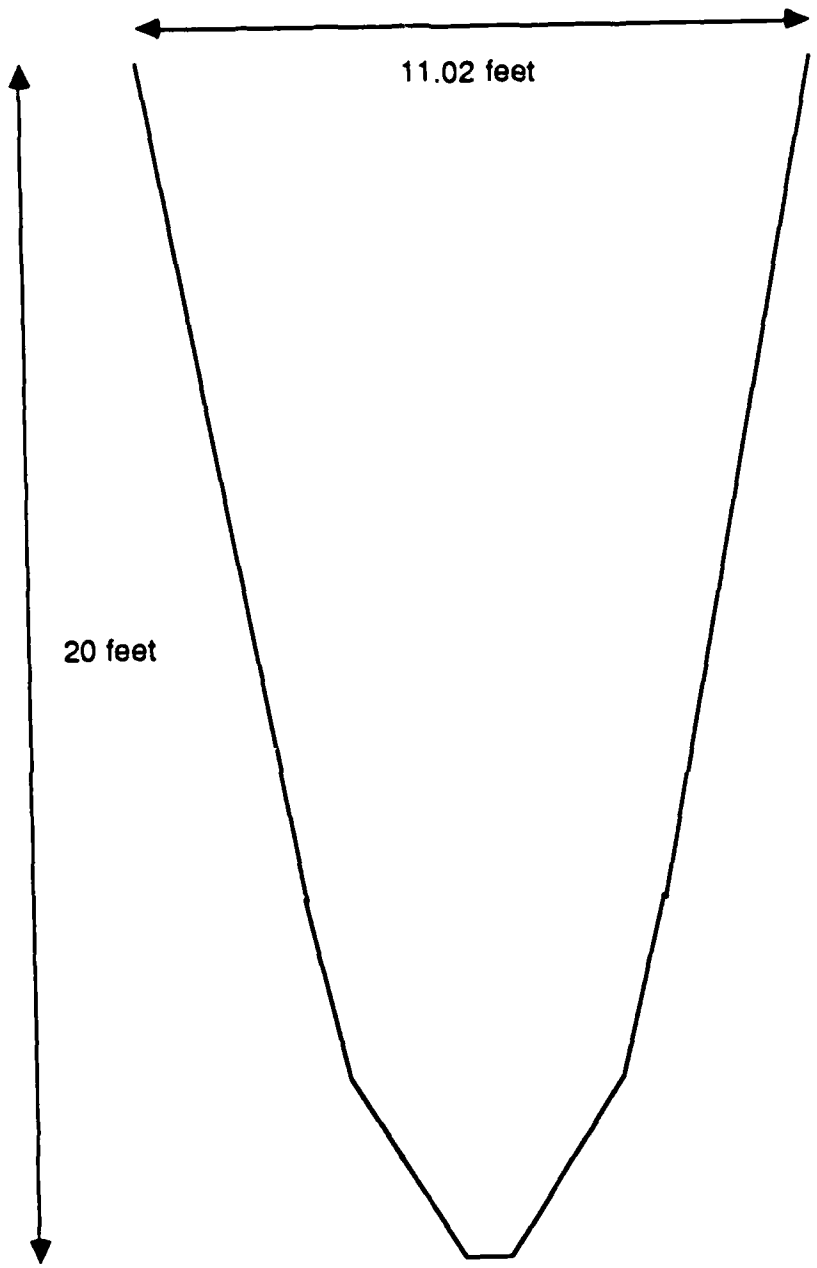

Figure 3. Typical TRS flame profile.

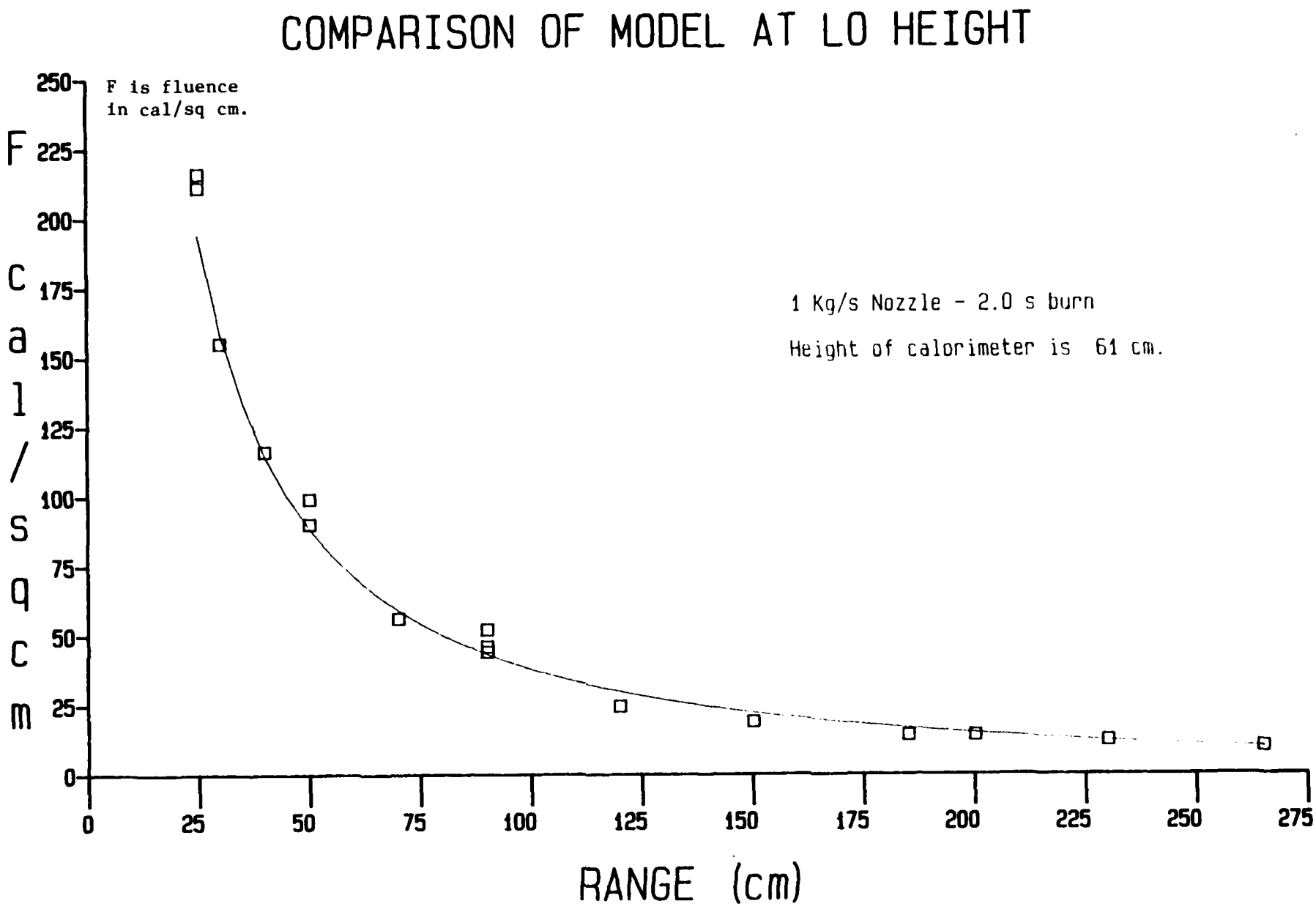

Figure 4. Comparison of model at low height.

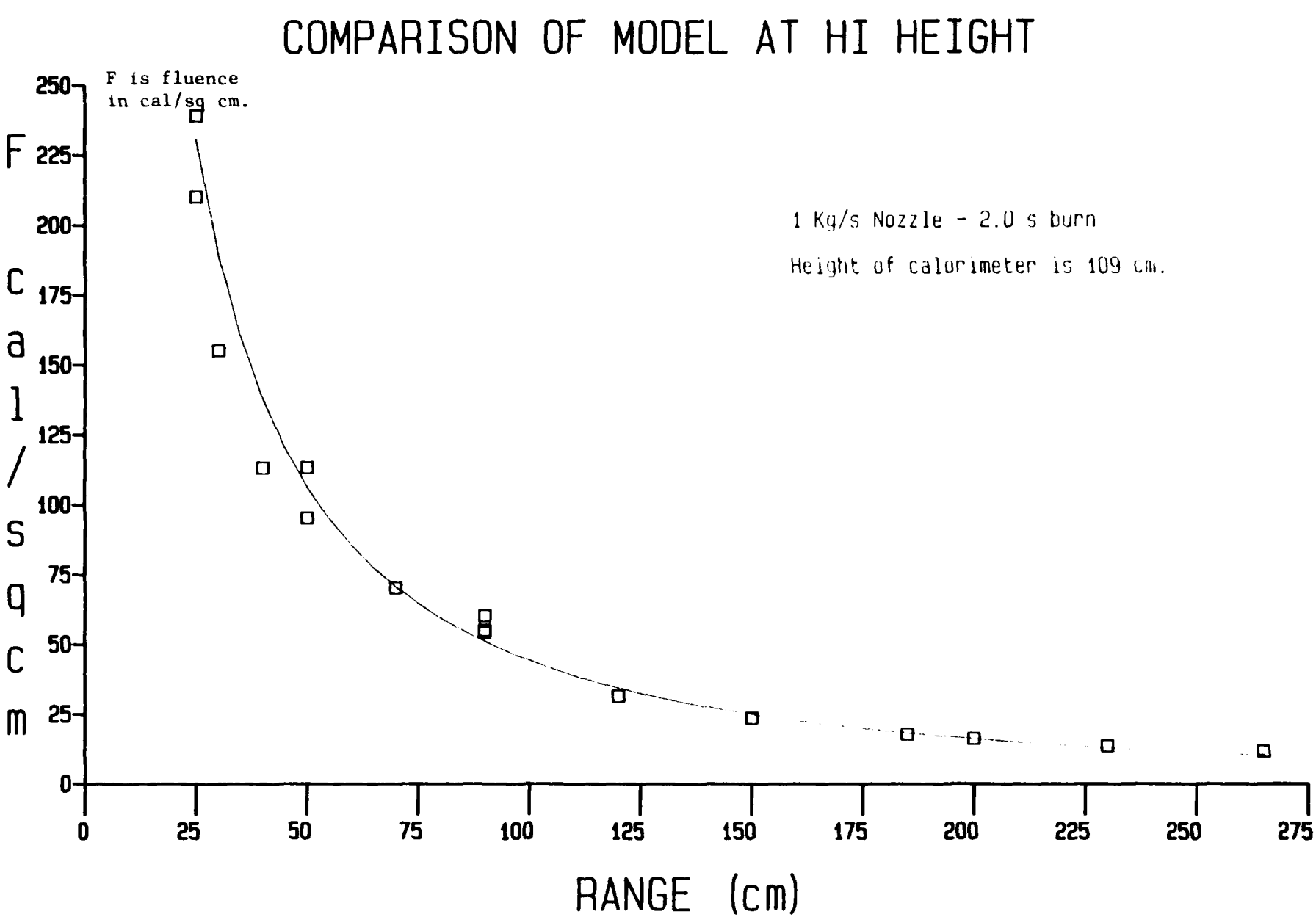

Figure 5. Comparison of model at high height.

SECTION 4

SPECTRAL AND TEMPERATURE MEASUREMENTS

Prior to this effort, the modeling effort relied principally upon calorimeter measurements from which flame characteristics had to be inferred. This is a difficult process because the TRS flame structure is influenced by wind conditions during a burn. The flame produced even by similar wind speed and direction does, in fact, have a stochastic component, although some think the flame is fairly repeatable. Unfortunately, there has never been sufficient opportunity to quantify this stochastic component.

Because a stochastic component does exist during any burn and the flames from any one nozzle are not really repeatable, it is impossible to obtain flame characteristics from what would otherwise be a minimum set of calorimeters. Instead, a statistically meaningful set must be used, which at the time of this effort had never been done. This lack of data has made the specification of the model's parameters imprecise.

Therefore, meaningful photographic measurements of the flame were obtained to guide the modeling activities. The advantage of scientific photography is to improve the bandwidth of information by literally orders of magnitude over what exists with calorimeters. Its primary disadvantage is that the optical wavelengths used only cover about 15 percent of the emitted energy bond, whereas the calorimeters measure about 90 percent of the emitted energy, i.e., about six times as much. Nevertheless, the information obtainable in the visible spectrum will be beneficial both to modeling efforts and to future planning of infrared measurements.

In order to conduct this set of scientific photography measurements, four cameras were used. Each was a Photosonic 4M type using half frame 35 mm format. The framing speed was 100 frames per second. The experiment consisted of photographing three TRS events and then selecting the most suitable for analysis. The analysis effort was restricted to 20 scans of film from each camera for one selected event.

Figure 6 shows a plan view of the layout of the cameras. The use of long focal length lenses and the large standoff distance (250 feet) was to simplify the analysis. The object shown as baffles is described in Section 5. The TRS array consisted of four nozzles placed along a line. The two inner nozzles were separated by 10 feet and the outer two were each 8 feet away from its nearest neighbor. Thus, the separation of the two outer nozzles was 26 feet. The cameras were placed on the opposite side of the SEA baffles (and other experiments) so that they would have a clear view of the flames.

The events photographed were: 5-19, 5-24, and 5-25. Event 5-19 occurred 13 April 1983 at 11:39 AM (MST). The wind speed measured near the ends of the TRS array (there are two permanently emplaced wind speed indicators at the FCDNA TRS site) was 1 and 5 miles per hour (MPH). No direction was recorded. Event 5-24 occurred 22 April at about noon. The wind was only recorded at one end of the TRS array; its speed was 9 MPH and its direction was ESE. Event 5-25 occurred the same day as 5-24 at about 5 PM. The wind speed was recorded as 15 and 18 MPH and its direction was WSW.

Cameras 1 and 2 were dedicated to making spectrographic measurements

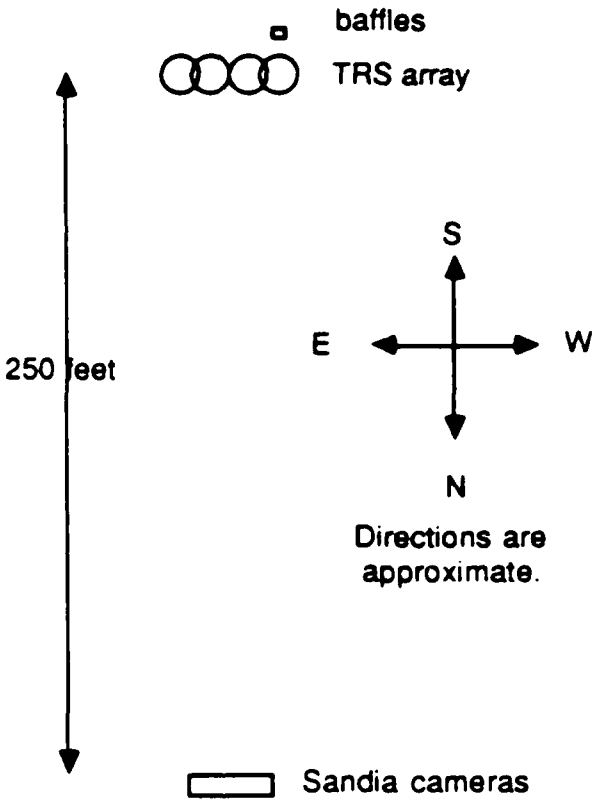

Figure 6. Plan view of camera layout.

each along one line. A slit acting as a stop allows a photograph to be made of the virtually one-dimensional line. A diffraction grating smears this image over the rest of the frame thus obtaining spectral information along the whole line. The alignment of the slit on the flame image in camera was chosen to obtain as much information over the entire flame as was geometrically possible.

Figure 7 shows this alignment for camera 1. Implicit in its choice is the assumption that each of the four flames will be similar. The idea is to obtain spectral information across the flame at different heights. If the flames are each axisymmetric about the plumb line above their nozzle and each nozzle produces essentially the same flame, then this diagonal line is similar to having diagonal measurements across the flame at six heights.

Figure 8 shows the slit alignment for camera 2. In this case we concentrated on measuring the spectral information along its axis. Our measurements provide us with detailed variations with height albeit, over one line. This camera was aimed at the same flame that the baffle experiment was measuring.

Camera 3 photographed the entire burning of the TRS four nozzle array at a very narrow waveband in the deep red to provide surface brightness information. These photographs provided quantitative information whereby surface radiating temperatures can be estimated, but also show details of the flames' structure in this waveband. Much of this information is useful for inferring some of the underlying physics of the TRS flame.

Camera 4 recorded the same information as camera 3, primarily as a backup system, but was lost on event 5-19.

Because of the performance of the flames in Event 5-19, it was the one analyzed even though camera 4 was lost on that event and the exposure was best on the last two events (it was good on all of them). The wind speed was the dominant factor in deciding what event to analyze. It appeared from the quick look of the three shots that the flames burn hotter on the upwind side of the flame, i.e., they produce higher radiance when viewed from the upwind side. Further, Reference II reports that they burn cooler on the leeward side; this effect is consistent with our baffle measurements of events 5-24 and 5-25. (Event 5-19 was not compared as will be explained in Section 5).

Parts of the following subsection were extracted from Reference 12, which was provided to SEA under subcontract; these extracted parts were edited by this author.

4.1 SPECTRAL AND TEMPERATURE DATABASE.

This section contains a brief summary of a database of thermal information as measured from one of the four nozzle TRS events, TRS 5-19. A significant, erratic wind condition existed during this event. The wind direction was predominately toward the camera systems and away from calorimeter sensors. This TRS event was a one second burn and the photographs show that the source was still very active at one and one-half seconds.

The camera station was located 250 feet away thus allowing the camera slit axes to be nearly normal to the plane containing the four nozzles of the

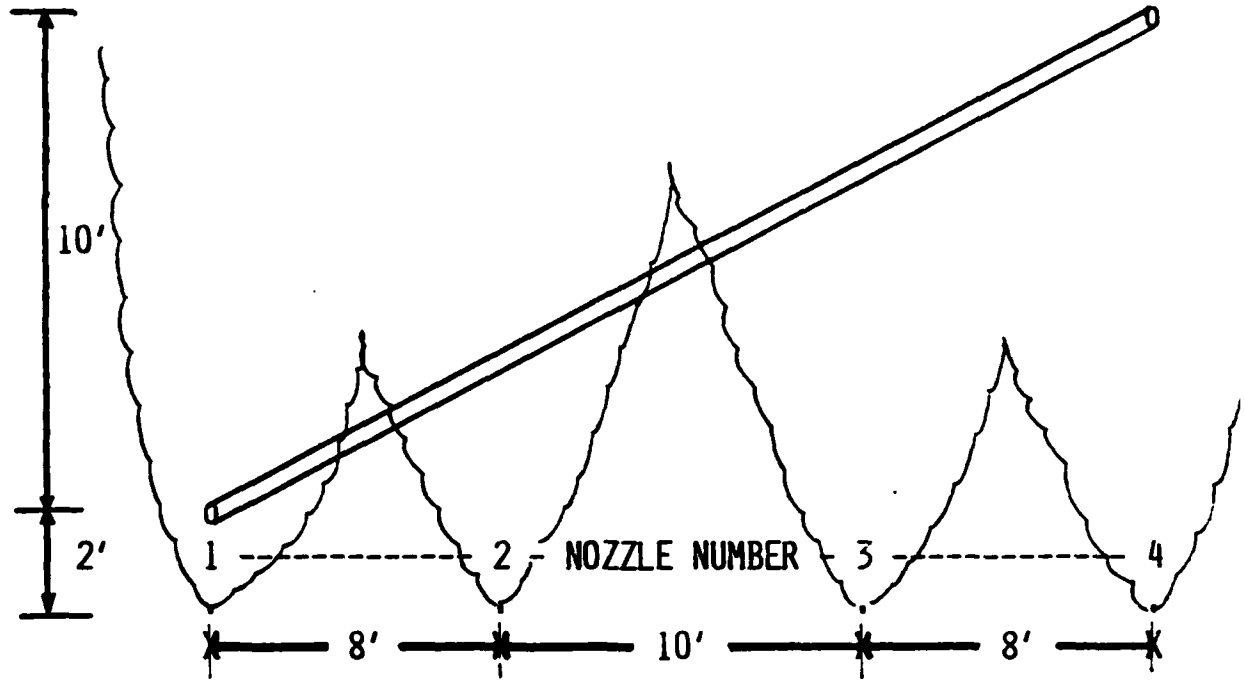

Figure 7. Camera 1 slit orientation on image.

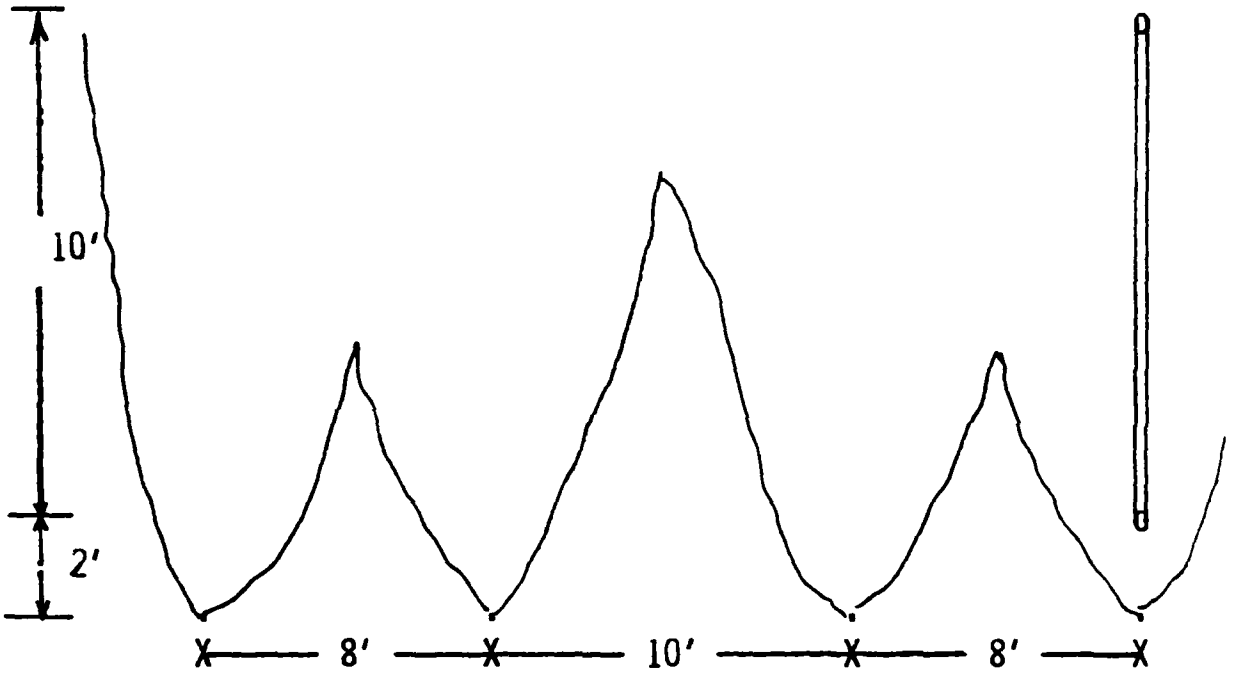

Figure 8. Camera 2 slit orientation on image.

TRS source. In this plane, the separations of the nozzles, as viewed (left to right) from the camera station were:

between nozzle 1 and 2 -- 8 feet
between nozzle 2 and 3 -- 10 feet
between nozzle 3 and 4 -- 8 feet

Nozzle 4 was nearest to SEA's calorimeter station.

Four camera systems were used to characterize the time-varying spectral and temperature variations of this four-nozzle source. Two pin-registered Photosonic 4M cameras, using a half-frame 35mm format, photographed selected segments of the luminous content of the source in the 400 to 700 nanometer waveband. Two other similar pin-registered Photosonic 4M cameras, using a half-frame 35mm format, photographed the brightness variation with time of the source surface. All four cameras ran at a nominal framing speed of 100 frames per second.

To allow analysis to yield photometric information, the film records were calibrated in the field through the same photographic recording system, by using an NBS-calibrated tungsten source set at a temperature of 2600 degrees Kelvin. Since the calibration source could not be located with respect to the camera system at the location of the TRS source, an optics correction factor of 0.88 was experimentally established for the bellows effect (i.e., required refocus changes needed to record the two sources). A framing speed variation film exposure factor of 1.22 was experimentally established. This allowed compensation of framing speed variation between recording of the event and the calibration source. The reduction of image size by the optical grating system was also measured. For the camera recording the vertical spectral variation, this image reduction factor was 0.71, and for the diagonal spectral variation, it was 0.78.

A mercury light source has very well-defined spectral lines. Such a mercury light source was also recorded in the field, on the event film records, through both spectral optic systems. Measurement of the position on-film of the images of these known, mercury spectral lines, established the wavelength versus film position calibration curve for each spectrometer.

These and other measurements were used to establish the optics and film calibration parameters, which were used to transform film image density and position variations to source surface radiance and position values presented in this data base. For convenience, this observed radiance is converted to black body temperature by Planck's law, which defines the spectral distribution of thermal energy at temperature T. The conversion scale is based on the Planck relationship between monochromatic emission power and the equivalent absolute temperature of a black body.

Some photographic images were documented in Reference 12. Some of these are included to help the reader understand what data are available. The data in the reference are presented in seven different sections. This report repeats what is said about each of those sections before showing some of the results. The following text, although slightly modified, can be found in the reference.

Section 1 (of Reference 12) contains selected results from ten frames

produced by two cameras which recorded the surface brightness variation of TRS 5-19. These are at 0.1, 0.2, 0.4, 0.5, 0.7, 0.9, 1.0, 1.1, 1.3, and 1.5 seconds. Time zero is taken as the first film image which registered observed light from the entire TRS unit.

Each time is described by a photograph and six graphic plots. The first plot shows the microdensitometer density representation of the film image produced by a (200 by 200 sampling) roster scan of the image. Each density sample was obtained by determining the transmittance on the film image of an area (a single pixel) of 50 by 50 microns. Since a 6 inch lens was used each pixel corresponds to a 1 by 1 inch square surface area on the TRS source. The roster scan was such as to sample (create a new pixel) every 2.25 inches on the source surface in both x and y directions. The vertical scale on this plot is such as to set ground zero of the TRS unit at 250 centimeters.

The next four plots are vertical temperature profiles at the center of the luminous region created by each nozzle. The horizontal scale of 200 pixels showing vertical height can easily be transformed to physical coordinates since this distance in physical space equals 1137.50 centimeters.

To allow these estimates of surface temperature using Planck's low the field camera conditions were purposely set to record surface brightness in a very narrow waveband (deep red). This was accomplished by filtering the light source prior to film exposure with a Kodak Wratten 92 filter. Thus the recorded surface brightness, as illustrated in the photograph, is limited to a small waveband with a peak effective wavelength of 650 millimicrons.

The sixth graph represents contour temperature plots over the entire luminous TRS surface. The contour temperature values indicated by letters A, B, C, D, and E, are determined by Planck's law from a measure of radiance. As indicated on the plot an emissivity of 1 is assumed since at this time emissivity of the TRS source is not known.

Two graphs are presented at the beginning of section 2 (of Reference 12). These are calibration graphs which allow transforming a density measurement on film to a radiance value and also of position on film into wavelength. The presented density log exposure curve is properly adjusted within the computer for variation of film response with wavelength prior to density conversion to radiance.

Sections 2, 3, and 4 (of Reference 12) present spectral measurements at different heights at one of three times (0.3, 0.5, and 0.8 seconds) as they have been measured by the spectrograph oriented in the vertical direction along the center of nozzle 4. Some photographs are also included to help understand the complexity of the data. A study of the photographs also reveals the presence of absorption lines which would not exist were the TRS a black body source. By comparison with the accompanying radiance plots it is clear that the higher wavelengths are recorded at the left of the spectral photographic records.

Section 2 (of Reference 12) presents spectral radiance and spectral temperature measurements as observed on the source in an area 2 by 2 inches square at heights of 0, 0.36, 0.61, 1.11, 1.36, 1.61, 1.86, 2.11, 2.36, 2.61, 2.86, and 3.11 meters above the ground surface. In this section these measurements are for the time of 0.3 seconds after start of event.

Section 3 (of Reference 12) presents similar data from the vertical spectrograph at a time of 0.5 seconds. Section 4 (of Reference 12) presents it at a time of 0.8 seconds.

Section 5, 6, and 7 (of Reference 12) present similar spectral information from the TRS 5-19 source as obtained with the diagonally oriented spectrograph. This spectrograph recorded data from the source along a slit oriented at 21 degrees at the horizontal. The low point of the slit was near nozzle 1 such that at the center of nozzle 1 the slit would sample at a height of 2 feet off the ground. This slit orientation sampled the source at the center of nozzle 4 at 12 feet above the ground. The graphs show the distance in meters above the ground and along the slit.

4.2 SUMMARY OF SPECTRAL AND TEMPERATURE DATA.

The results for 0.9 seconds were selected from the documented data for brightness variation since they show a well developed flame and the photograph (Figure 9) from camera 3 is quite clear. In fact, the SEA baffle fronts can be seen. Also included is a plot (Figure 10) of microdensitometer density representation of the film image (200 by 200 sampling). The image area was 50 by 50 microns or 1 by 1 inch at the flames. A "pixel" was assigned at every 2.25 inches. Ground zero was at 250 cm on the plot of the image. One plot of vertical backed-out temperature profile is shown as Figure II for one nozzle along the flame's axis. The same pixel spacing was used. The data are limited to a narrow waveband at 650 nanometers. Figure 12 shows a plot of "temperature" contours. Five contours are shown: 2070, 2380, 2700, 3010, and 3330 degrees Kelvin. In order to obtain this plot an emissivity of one was assumed. The actual emissivity is not known, and furthermore, this effort has shown that it is spectrally dependent.

Only a few figures are shown of the documented data for spectral measurements because of the need for additional interpretation. The data shown are illustrative and were extracted from the reference, which includes times 0.3, 0.5, and 0.8 seconds for both orientations: vertical and diagonal. The spectral radiance was measured from 400 to 700 nm, but is only plotted from 450 to 700 nm. The sample size at the flames was a 2 inch square. The reference included plots at various path length, which is height for the vertical orientation. For the vertical orientation the heights were 0, 36, 61, 111, 136, 161, 186, 211, 236, 261, 286, and 311 centimeters above the ground surface. The diagonal orientation was inclined at 21 degrees; it intersected nozzle 1's centerline 2 feet above the nozzle and intersected nozzle 4's centerline at 12 feet. The positions on the diagonal paths were: 30, 95, 160, 225, 290, 355, 420, 485, 550, 615, 680, 745, and 810 cm. The corresponding heights relative to a line 2 feet above the nozzles are: 11, 36, 61, 86, 111, 130, 161, 180, 211, 230, 261, 280, and 311 cm.

These data were obtained by scanning the film in either of two directions as shown qualitatively as Figure 13. The examples of what is available are shown as Figures 14 through 16.

Figure 9. Photograph of 5-19 at 0.9 seconds.

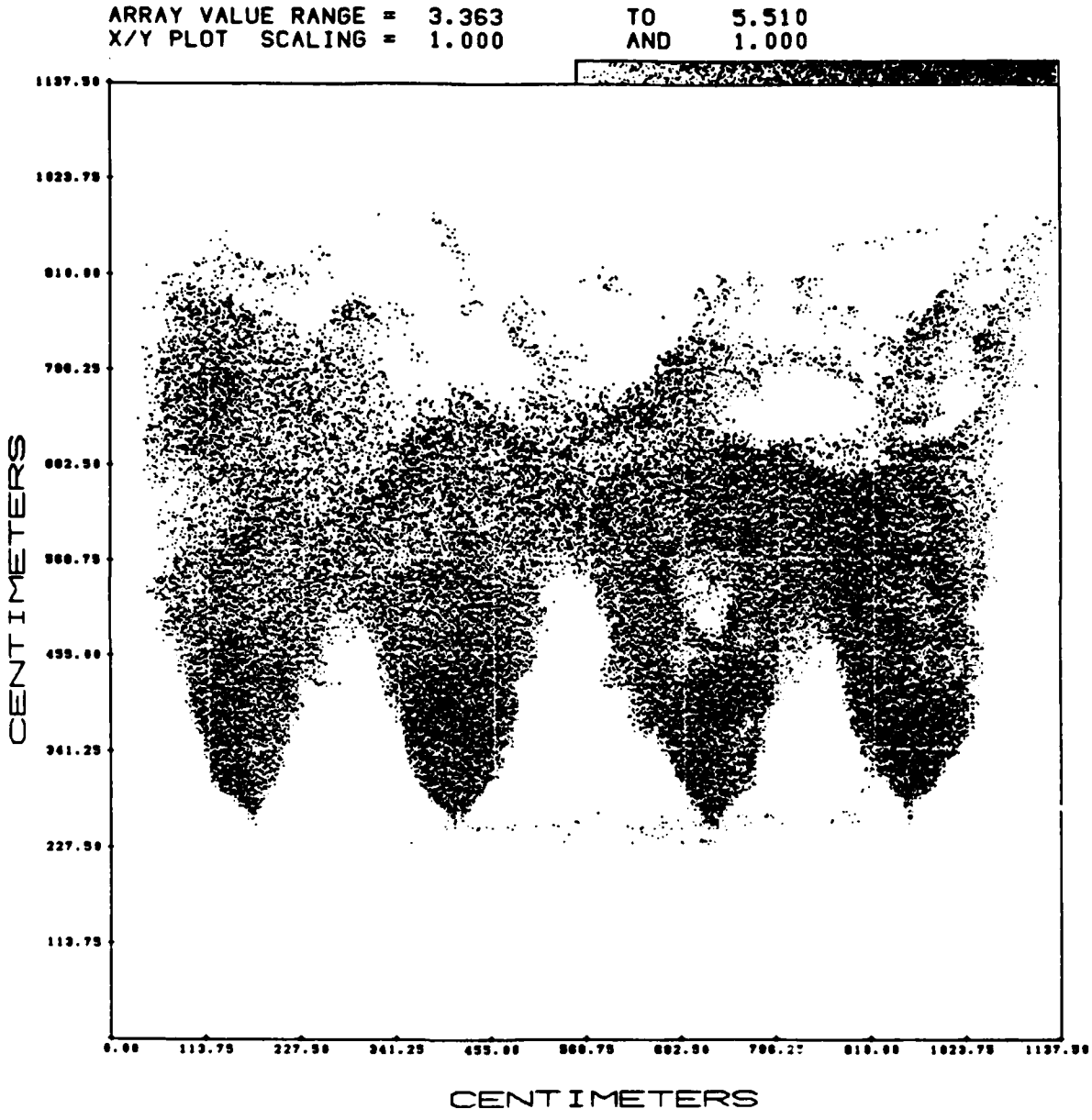

Figure 10. TRS 5-19 +0.9 SEC. RAD. 650 MU.

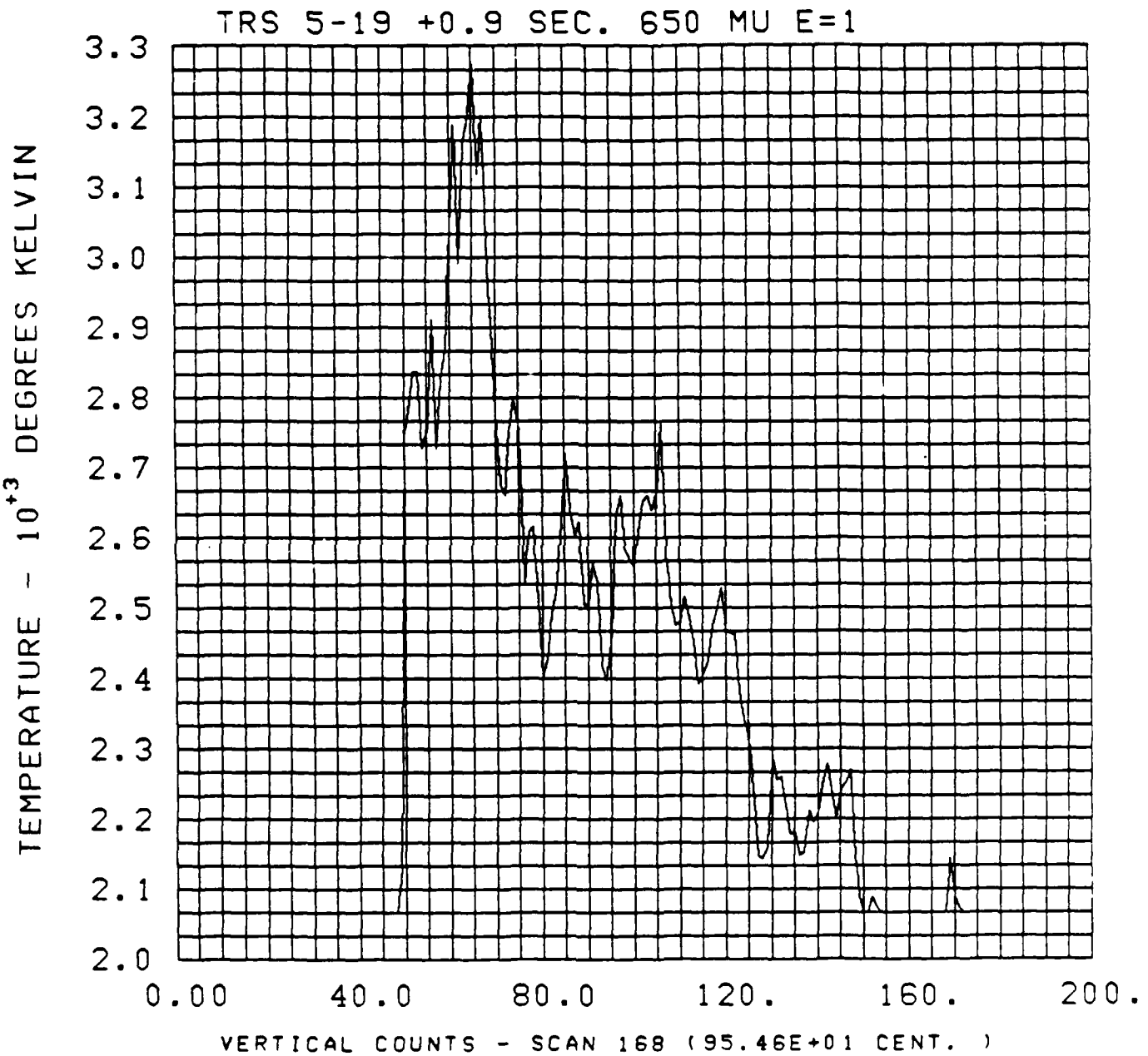

Figure 11. Temperature profile along scan.

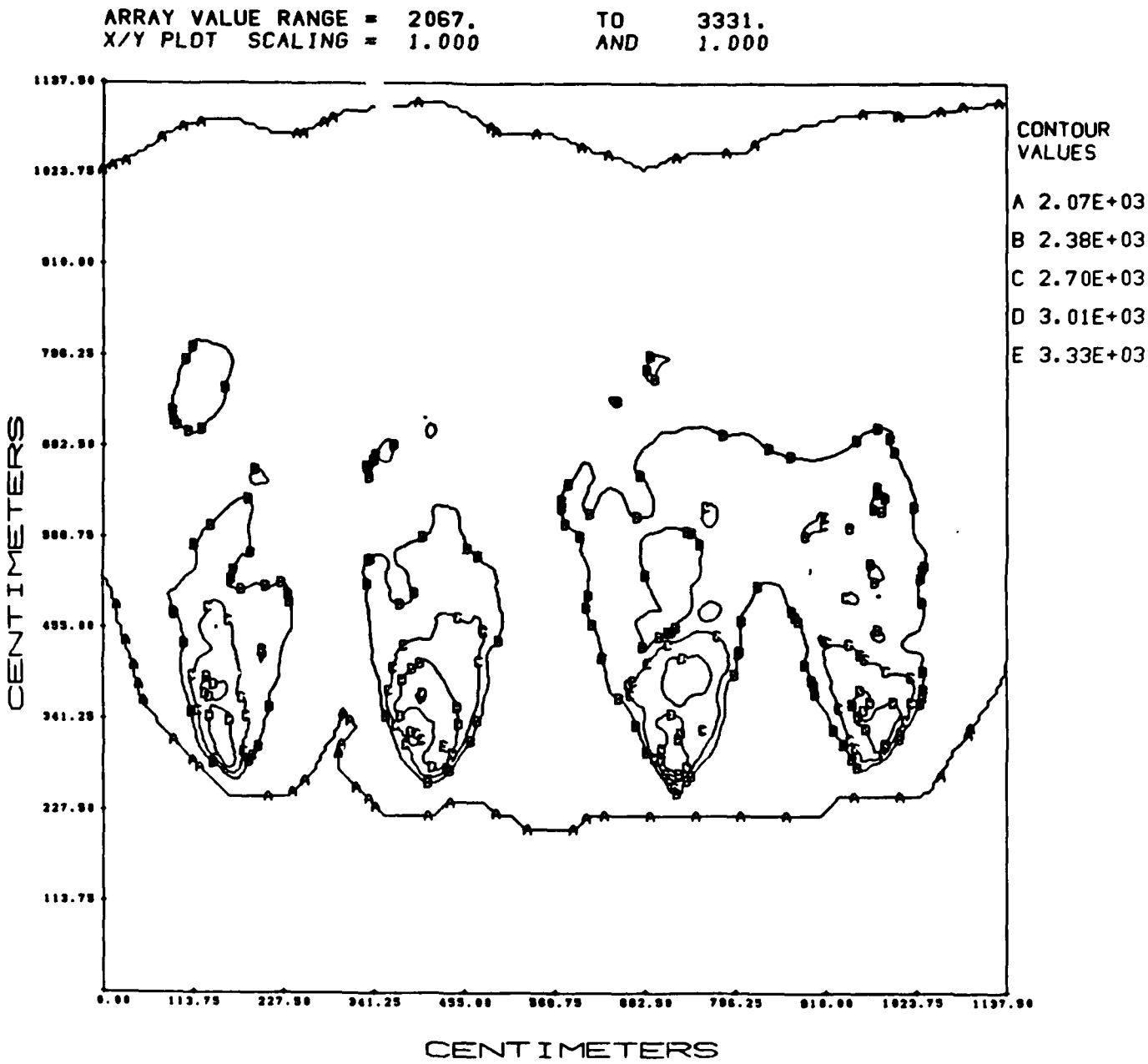

Figure 12. TRS 5-19 +0.9 SEC. DEG. K 650 MU E=1, temperature contours.

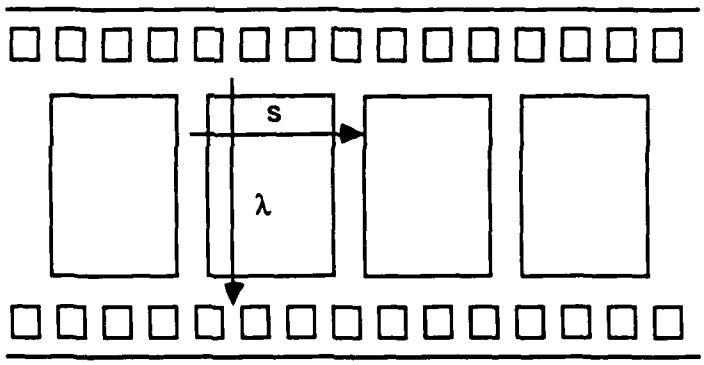

Hypothetical measurements for both scans.

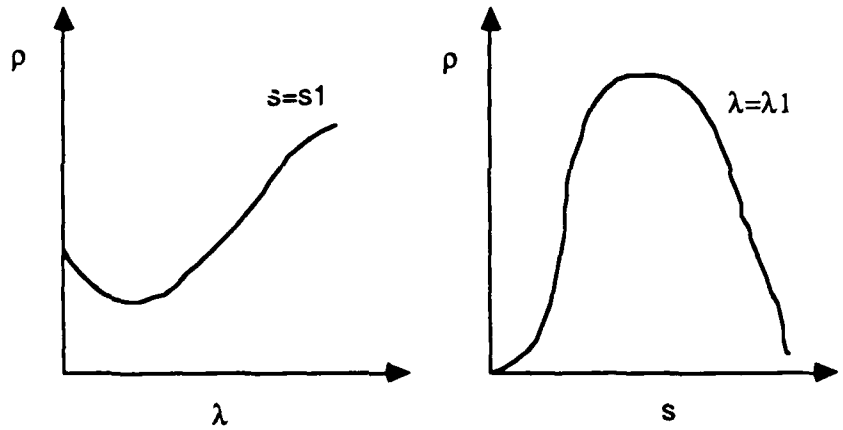

Figure 13. Scan lines used for analyzing camera 1 and 2 data.

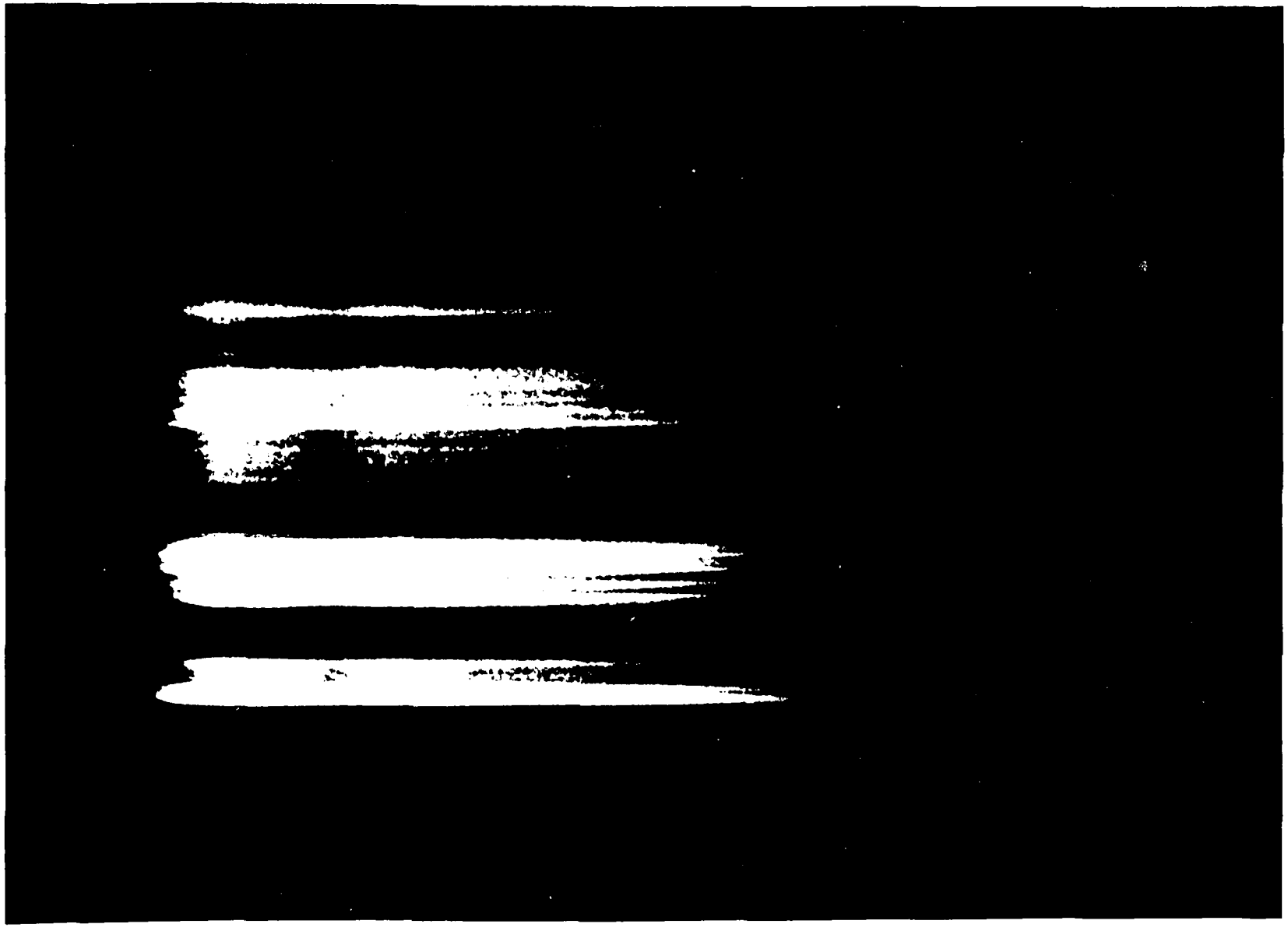

Figure 14. Photograph of spectral measurement.

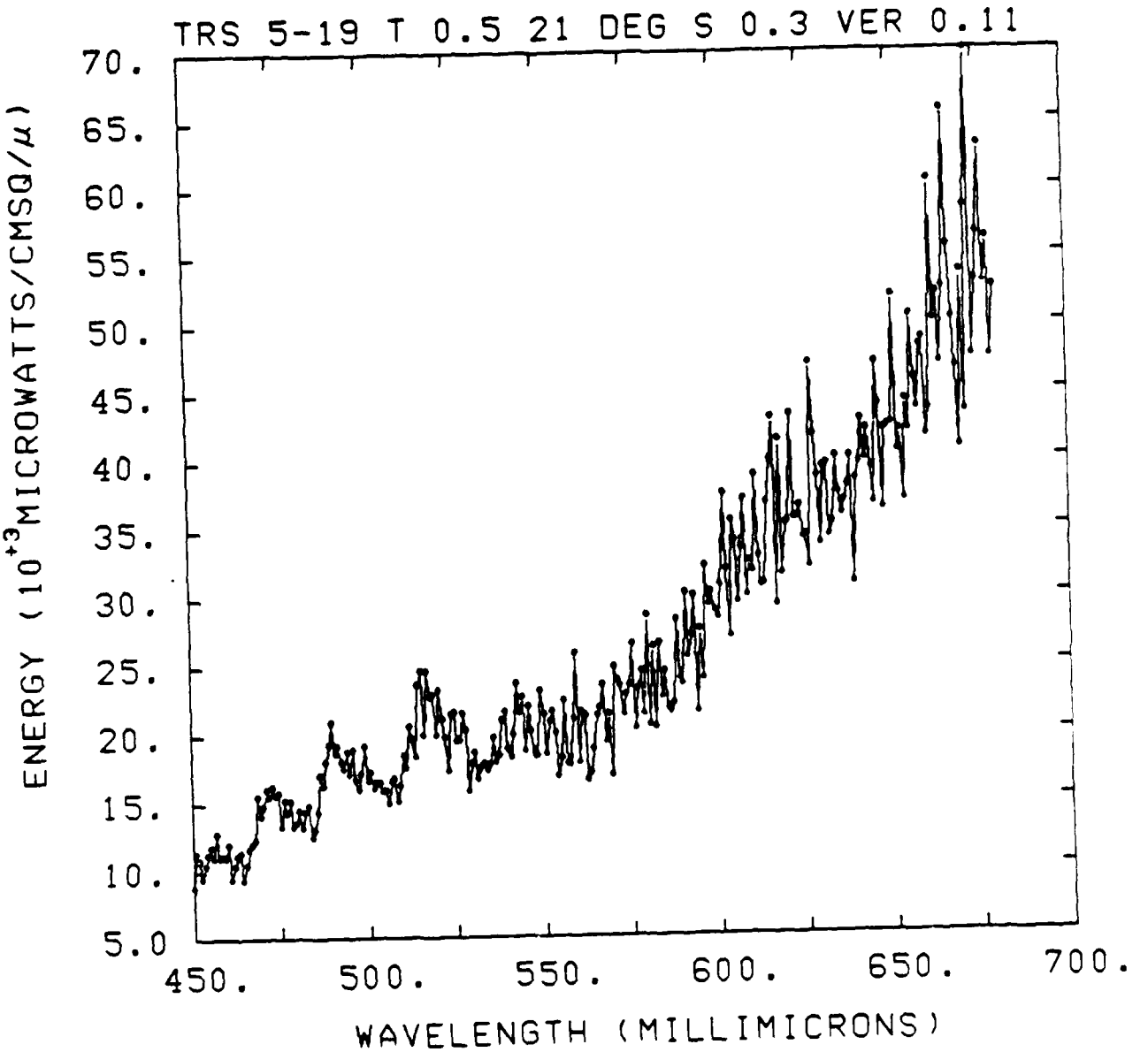

Figure 15. Result from spectral measurement in energy units.

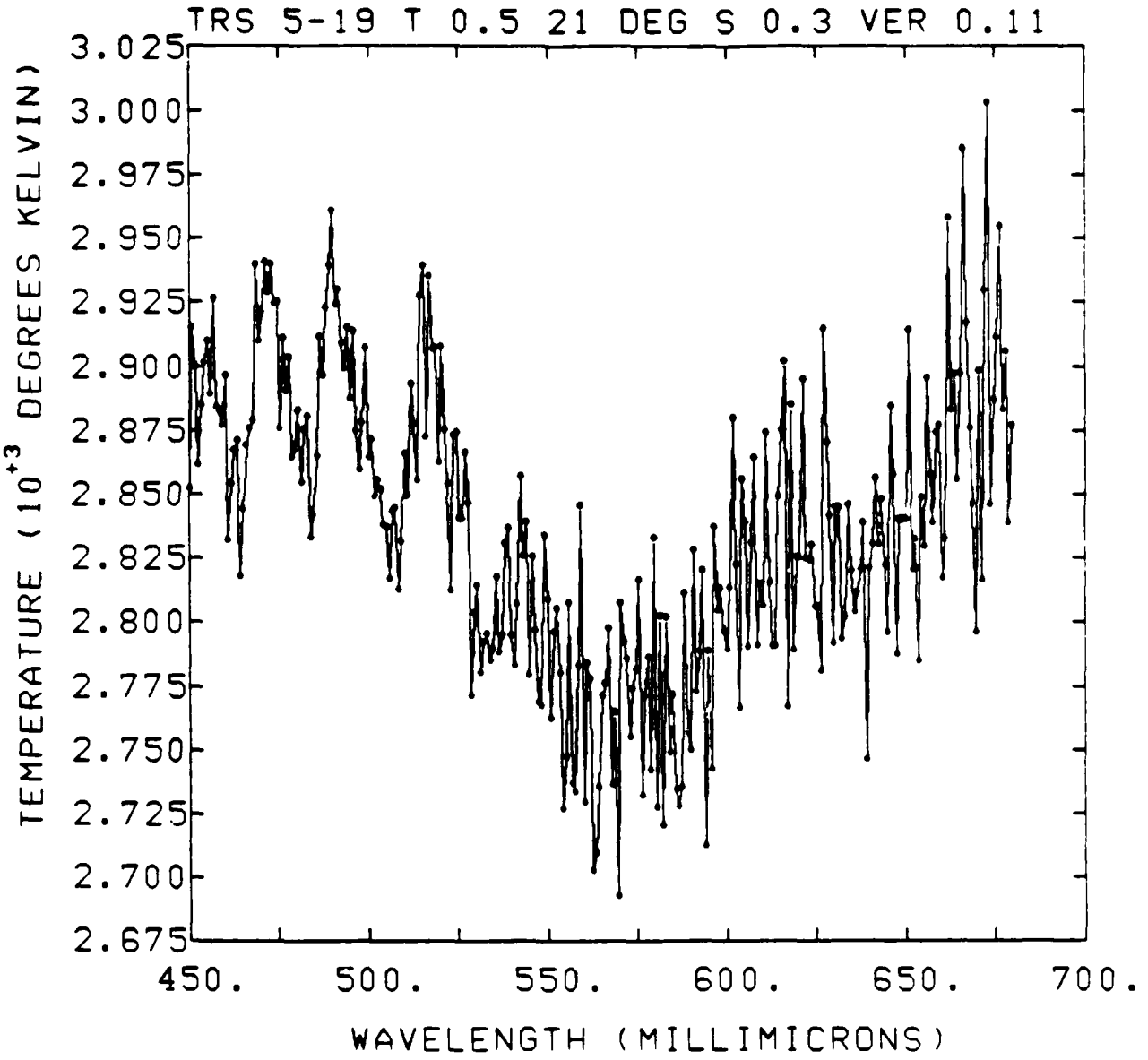

Figure 16. Result from spectral measurement in temperature units.

SECTION 5

DIRECTED FIELD-OF-VIEW RESULTS

The original point source TPS model had been improved through several iterations to reach the inverted cone model that existed at the start of this effort. Model improvements had generally been supported by the limited data acquired on TRS test firings. Even with those improvements, there was still significant differences between predicted and measured irradiance levels at some locations in front of a TRS. These differences can have several sources including both model deficiencies and measurement error. These are related because the model has been developed and validated with the aid of the existing measurement data base. This database was small and therefore errors within it can significantly impact model parameter determination.

It is however, just such a detailed model which must be developed for the LB/TS. At the time of this effort the TRS had only been used in field experiments. In that case, the only reflective surface of note is the ground. In the LB/TS the TRS will be largely confined and the walls of the structure may significantly influence the thermal load delivered to a target. Additionally, a detailed knowledge of TRS source characteristics could assist in the selection of LB/TS construction materials and also perhaps in physical design. To support the development, and validation, of a detailed model, the TPS must be characterized with a higher degree of spatial and spectral resolution.

The objective of the directed field-of-view calorimeter testing was the acquisition of source-resolved irradiance data. The approach was to design, fabricate, and field calorimeter baffles that limit the calorimeter's field-of-view. Six of these baffles (or collimators) were built and fielded. Unfortunately, review of the data from the first TPS event revealed that the design of the baffles was flawed. Two modifications were made in time for subsequent events. The data then obtained agreed fairly well with the existing model, except that the maximum peak power per unit height occurred at 5 feet rather than the predicted height of 7 feet. A later improved model that resulted from this effort agrees with the measured value of 5 feet.

The objective has been partially met with the acquisition of TPS source data using restricted field-of-view calorimeters. The field-of-view was restricted by using baffles which limited the TPS area "seen" by the calorimeter active element. (Additional data were also obtained with radiometrically calibrated scientific photography as described earlier in Section 4).

Calorimeters without baffles record the integrated irradiance over their field of view (up to pi steradians). As shown (Figure 17) for two example calorimeters and a model of the flame as a set of point sources (pretending the ground plane can be treated as if it specularily reflects the sources above), all emitters add to the integral. As one extreme example, consider when data are available only at two locations. It is impossible to determine the distribution of the energy in height because there are more variables than known quantities. If on the other hand you restrict the solid angle viewed for each calorimeter (as shown in Figure 18) you can at least determine the contribution from each of those parts of the flame. Increasing

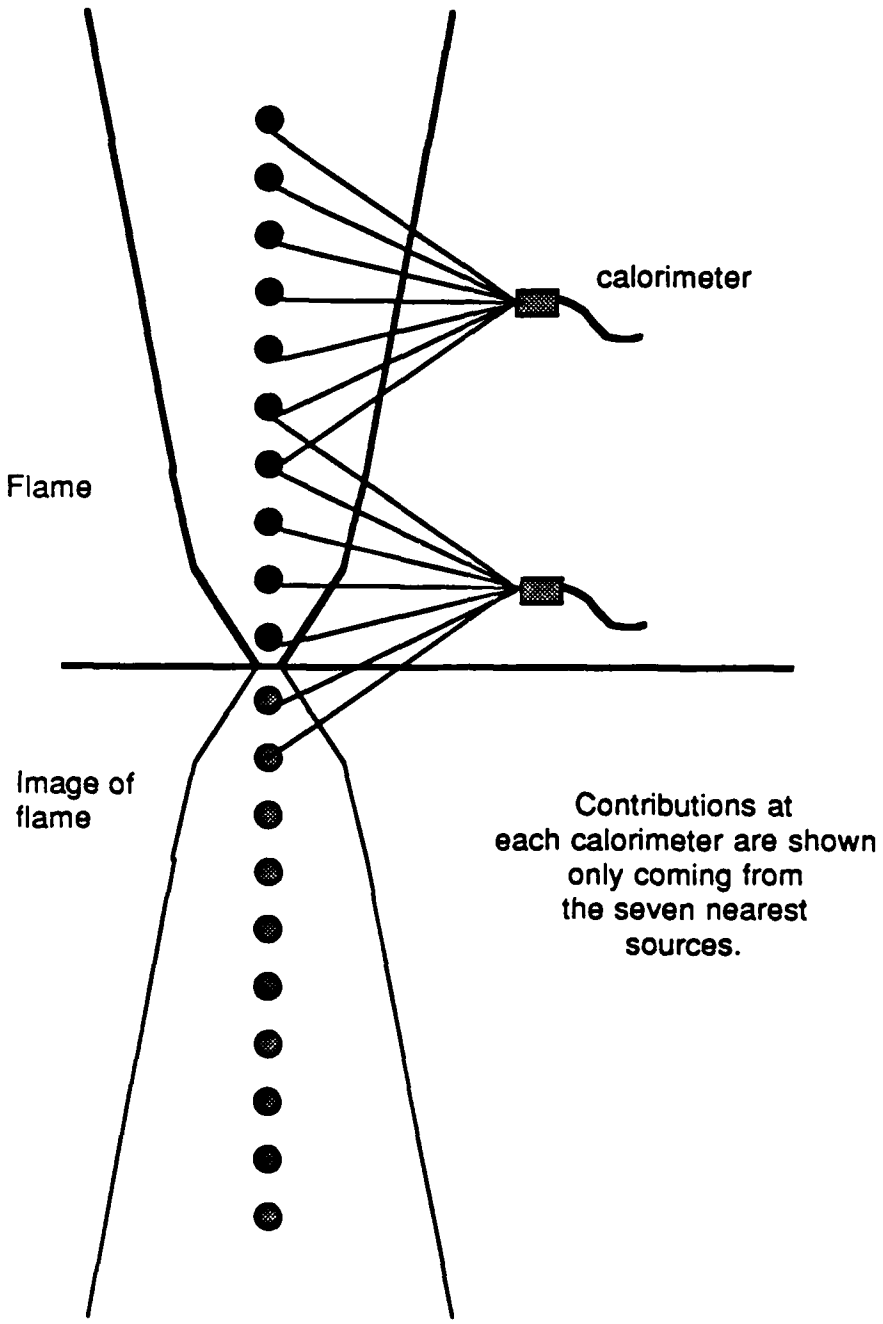

Figure 17. Pictorial of many sources on two calorimeters.

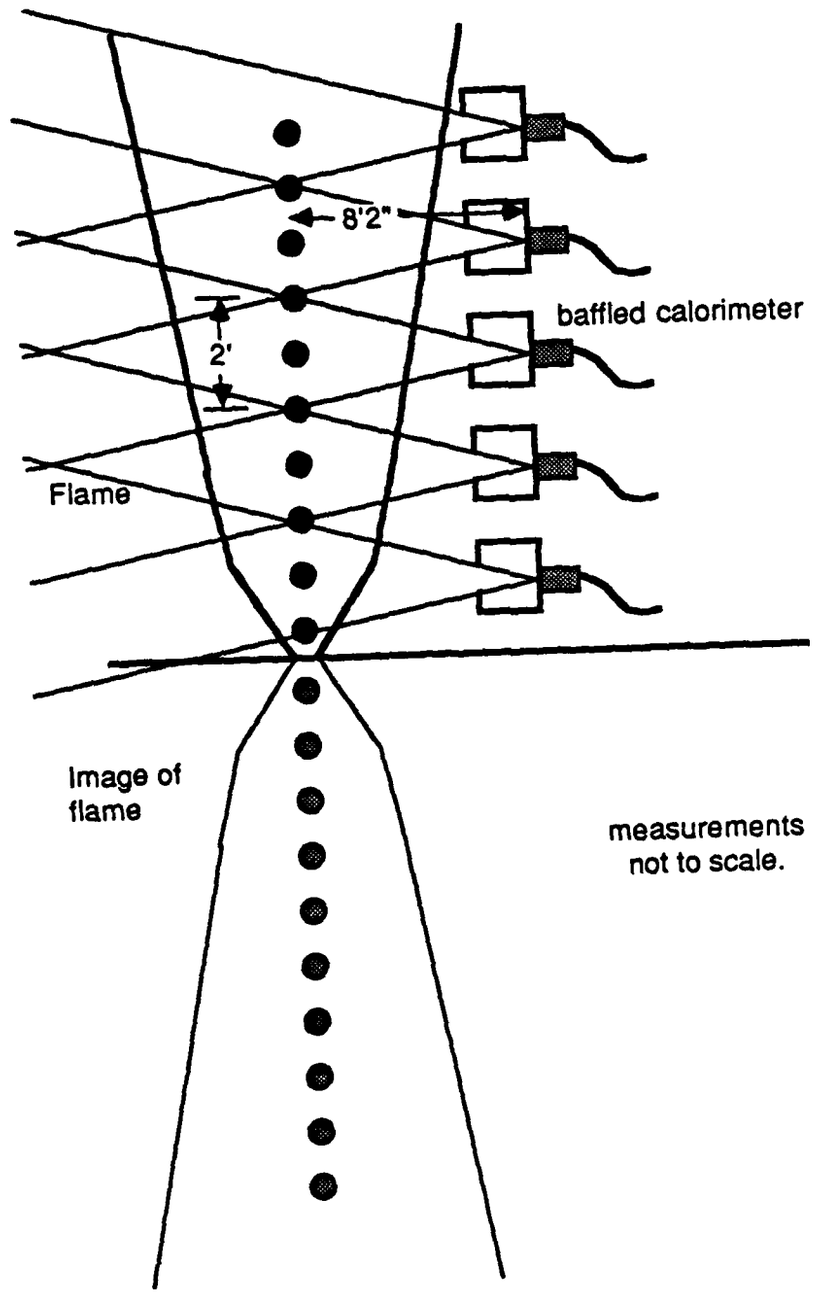

Figure 18. Pictorial of sources onto baffled calorimeters.

the number of the limited field of view calorimeters to observe the important parts of the flame unambiguously determines the necessary information.

These data were acquired during TRS firings (see Table 2) conducted the weeks of April 13, 1983 and April 20, 1983.

The results for the baffled calorimeters are summarized here. A crude approximation of the height dependency of maximum power per unit length of flame was obtained. Data collected on Event 5-19 (6 measurements) were corrupted by deficient collimator design. Measurements were made during events 5-22 and 5-23 at three heights: 5, 7, and 9 feet. The results from 5-23 were about 30 percent higher than those from 5-22. Event 5-23 is believed to be better because the wind speed was low. Measurements were made during events 5-24 and 5-25 also at three heights: 1, 3, and 5 feet. Event 5-24 is considered the better because the wind speed was lower. Finally, measurements were made during events 5-26 and 5-27 also at three heights: 9, 11, and 13 feet. Since these calorimeters were fairly high, flame products were deposited on most of the baffles during the burn. The 13 feet station during Event 5-26 was coated with these flame products and all stations were coated during Event 5-27. The experiments and data are described in more detail below.

5.1 BAFFLED CALORIMETERS.

Figure 19 is a schematic of the approach used wherein the outer baffle was sized to limit the calorimeter field-of-view to a two foot high by six foot wide area in a vertical plane through the TRS nozzle. Internal baffles are for stray radiation rejection. The areas viewed on the TRS are shown in Figure 20.

The diameter of the can is 8 inches. The depth from the first slit to the calorimeter's sensing surface was 8.17 inches. The three partitions interior depths were each 2.6 inches. Slit 1 was 2 inches high by 6 inches wide. The approximate image area was 2 feet by 6 feet since the distance from the four flame symmetry plane to the calorimeter was 8.17 feet (8 feet 2 inches) by design.

5.2 CALORIMETER MEASUREMENTS.

The first set of measurements made unfortunately have limited utility. This is because an unforeseen mounting problem prevented the use of premade baffles and the internal sides were not blackened. The effect was to allow too much internal radiation scattering into the calorimeters sensing surface. The measurements made during that series of tests are high and the lack of adequate stray radiation rejection seem to explain those results. The second set of data was acquired with a modified set of baffles, and more accurately record the data that were to be measured. Additionally, scientific photography were fielded on some of these events and there is therefore additional data available for analysis and correlation. For these reasons, the second fielding exercise is emphasized below.

These measurements were made as add-on experiments to other primary ones, and as such only three calorimeters were made available for data acquisition during each event. To assure full vertical coverage of the flame, six sets of data were acquired with repeated measurements for repeated fires.

Table 2. Directed field-of-view calorimeter testing.

Event no.	Heights (ft)	Comment
5-19	1, 3, 5, 7, 9, 11,	11' primary & secondary lost. All stations used bare galvanized steel. Low wind (W 1-5).
5-22	5, 7, 9,	High wind (SW 10-13).
5-23	5, 7, 9,	Low wind (S 4-5).
5-24	1, 3, 5,	Moderate wind (ESE 9).
5-25	1, 3, 5,	High wind (WSW 15-18).
5-26	9, 11, 13,	Top buffled coated.
5-27	9, 11, 13,	All baffles coated.

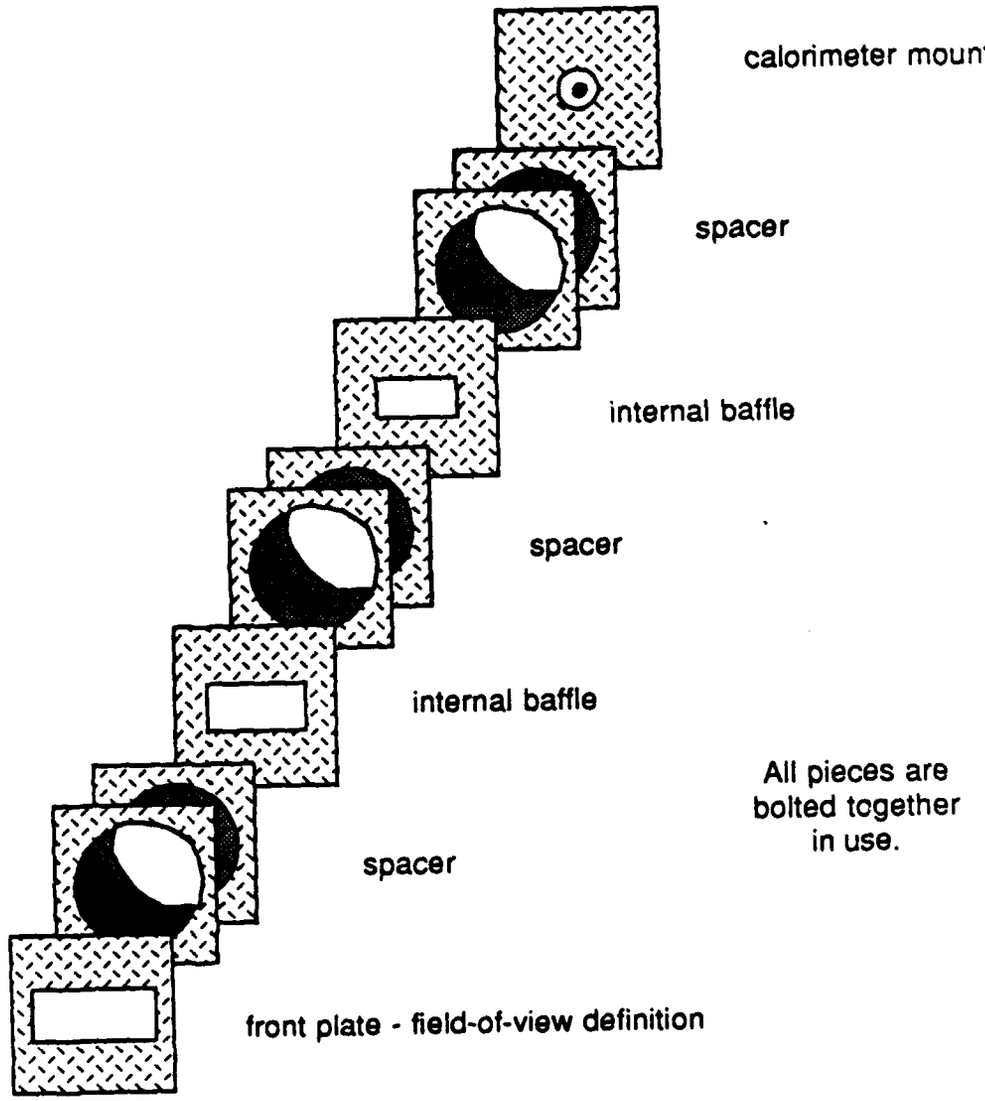

Figure 19. Baffle schematic.

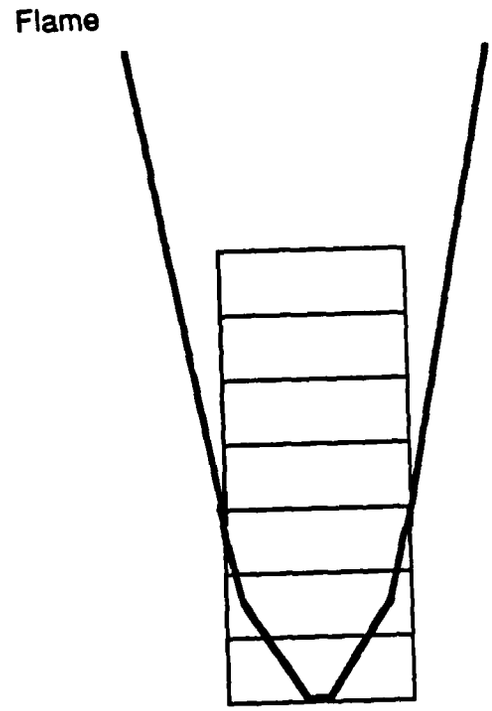

Figure 20. Sampled areas on TRS flame.

and with data overlap to assess internal consistency in the data set.

The calorimeter data acquired on these events is summarized in Table 3 and in Figure 21 and 22. The data have been presented in two different ways in the figures. In Figure 21, observed peak flux was obtained from flux plots generated at the TRS site and with calorimeter calibration data provided by the manufacturer. Similar data are plotted in Figure 22 except that here measured fluences for the nominal three and one-half second burns are plotted. Note that if the TRS source were non-varying and uniform, then the ratio of fluence to flux should be exactly the three and one-half second burn time. It can be seen from the ratios summarized in Table 3 that this is not the case.

Although some general trends and patterns can be seen in Figures 21 and 22, it is also obvious that there is substantial variability in the data.

Table 3. Calorimeter data.

Event no.	Calorimeter no.	Height (ft)	Peak Flux	Fluence	Ratio (Fluence/Flux)
5-22	1	5	3.25	9.57	2.94
5-22	2	7	2.95	7.95	2.69
5-22	3	9	2.52	6.40	2.54
5-23	1	5	4.64	13.34	2.88
5-23	2	7	4.30	10.90	2.53
5-23	3	9	3.15	10.87	3.45
5-24	1	1	1.48	4.35	2.94
5-24	2	3	3.90	11.20	2.87
5-24	3	5	4.58	13.72	3.00
5-25	1	1	1.42	4.41	3.11
5-25	2	3	2.47	7.83	3.17
5-25	3	5	2.35	6.85	2.91
5-26	1	9	1.33	2.90	2.18
5-26	2	11	1.18	1.47	1.25
5-26	3	13	0.63	0.57	0.90
5-27	1	9	1.42	3.13	2.20
5-27	2	11	1.00	2.59	2.59
5-27	3	13	1.03	1.77	1.72

Under the same conditions, a reproducible source would have made a consistent set. All of the data should have tied together at the five and nine foot locations. Instead, these data scatter by factors of two to four.

The winds during events 5-25 through 5-27 were significant and

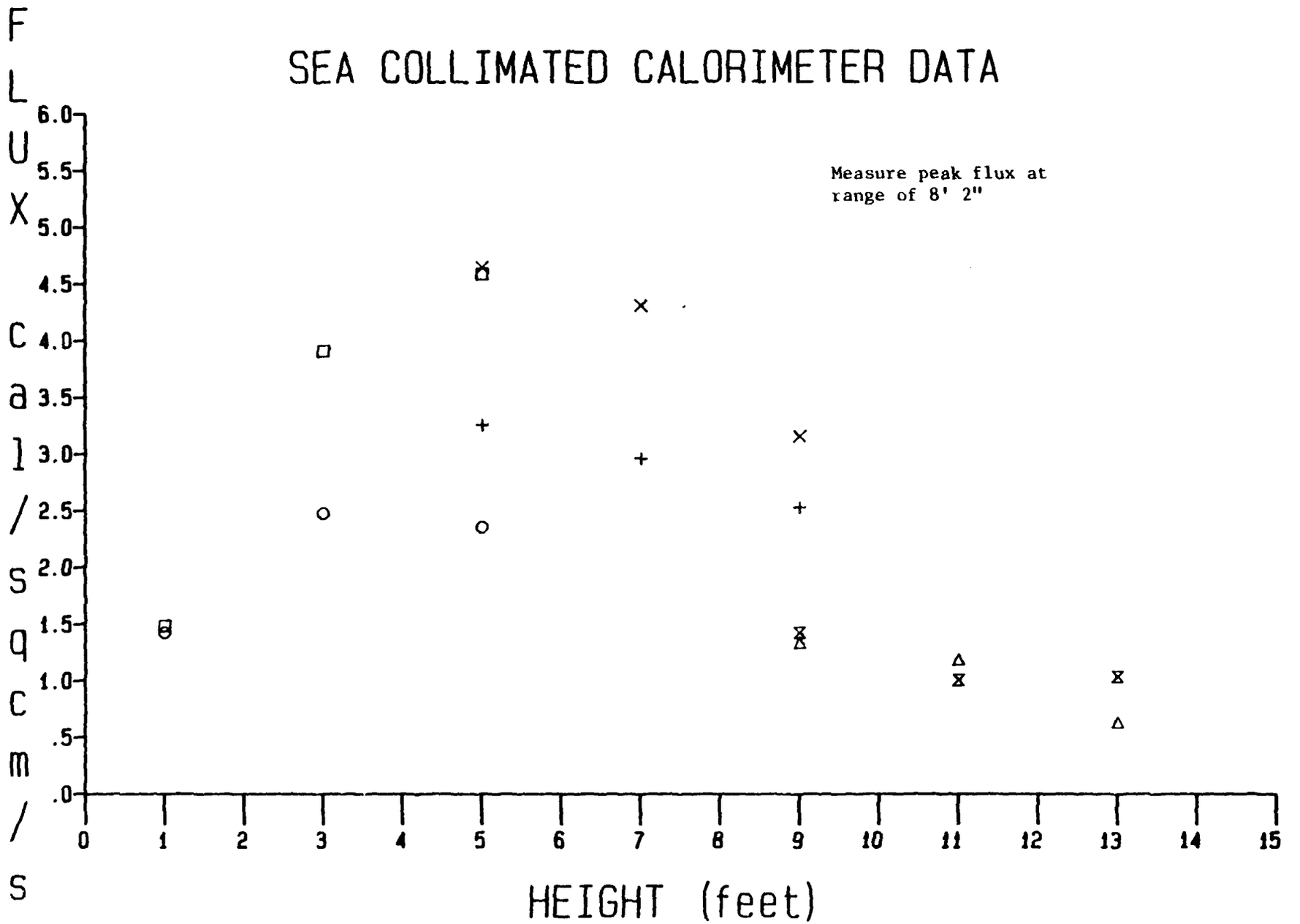

Figure 21. Results from baffled calorimeters (peak flux).

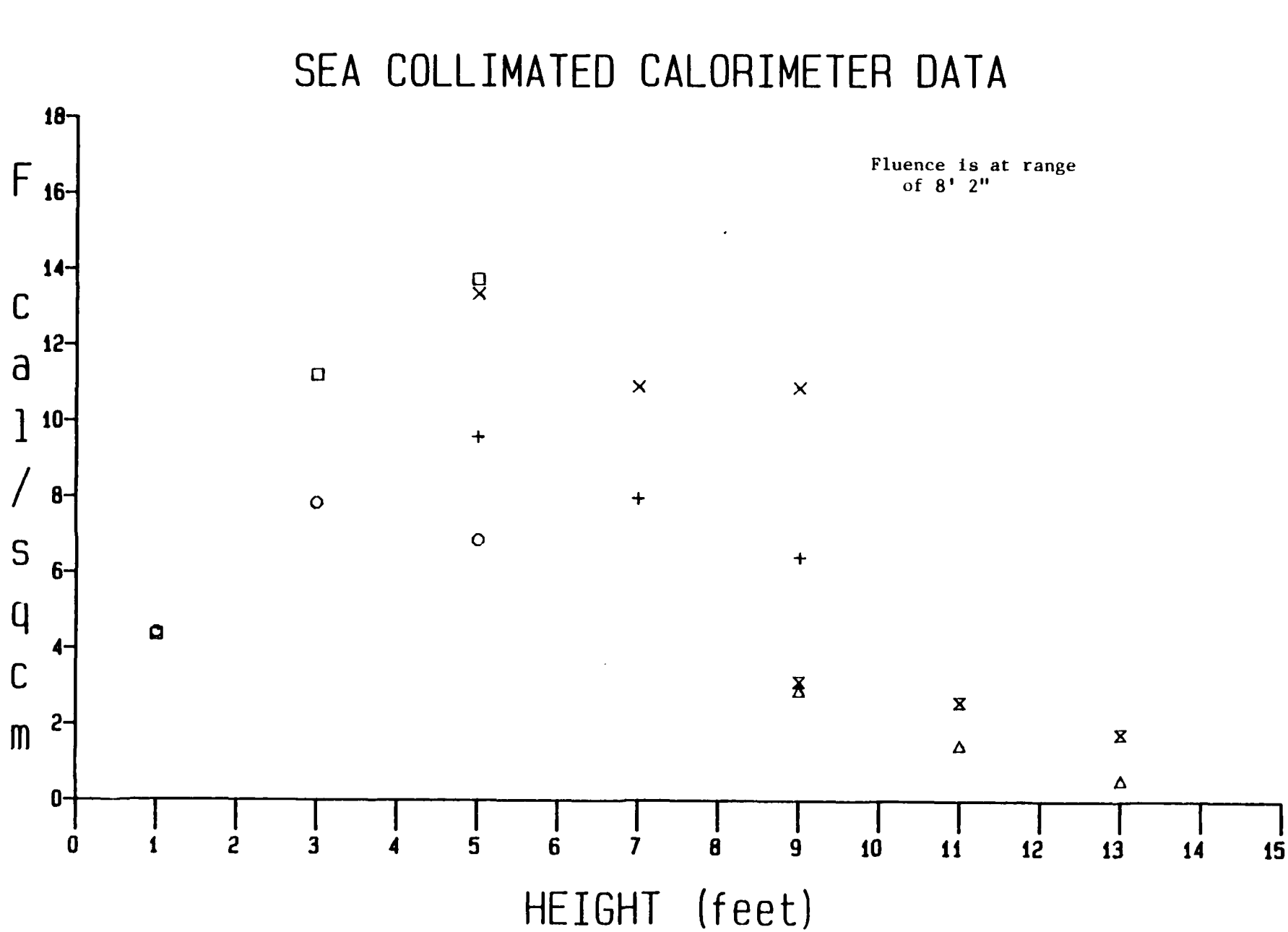

Figure 22. Results from baffled calorimeters (fluence).

blowing towards the calorimeters. As such, presumably aluminum oxide combustion products tend to obscure the flame and the net result is anomalously low data such as seen on 5-26 and 5-27, and the evident lowering of levels at 3 and 5 feet for 5-25. It is possible that scaling of these data, accounting for wind effects, would generate a self consistent data set, but the scaling factors, and their application, have not yet been identified. Presumably, this could be remedied given sufficient measurements.

Much more desirable, would have been the use of larger numbers of calorimeters to generate more data points for each event, thus providing more reliable height profiles. The problems of data matching and interpretation would then be minimized.

5.3 ANALYSIS METHOD FOR INTERNAL SCATTERING.

As has been stated earlier, two problems existed when the first measurements were made with the baffled calorimeters. These caused too much energy to be scattered internally into the calorimeter's sensing surface thus masking what we were trying to measure. The fluxes being measured were much higher than expected based on model calculations. Analysis led to the necessary baffle design changes.

Writing an energy balance for each compartment within the baffle provides a simple model for estimating the relative contribution from the undesired internal scattering signal compared to the directly incident flux. This model is based on initial conditions determined by geometry, wall absorptivity, and model predictions for both the incident flux at the entrance slit and that incident directly onto the calorimeter's sensing surface. Solving the resulting equations parametrically for plausible initial conditions quickly leads to the conclusion that the baffle should have at least three internal compartments given the sizes in the original design and that the baffle walls should be made to be reasonably absorptive.

The simple model built to perform the analysis to improve the baffle design is based on a physical interpretation as follows. The baffled calorimeter is similar to the conceptual cross-section view shown in Figure 23. The essential features are that there are a number of compartments, each having an entrance and exit, although some of the photons will exit an entrance and enter an exit. The exit of the last compartment is the calorimeter's sensing surface. Each internal wall has some absorptivity. Photons entering the system through the entrance slit of the first compartment can either encounter a wall or exit the compartment. Those encountering a wall will either be reflected or absorbed. Those that are absorbed will not be considered further (the heating of the wall and any subsequent reradiation is ignored). The reflected ones, however, can be sent back to the outside slit (and leave the system), or they can encounter the wall, or they can pass from compartment 1 to 2.

Similarly, photons move through compartment 2 to compartment 3 and sometimes back into compartment 1. Photons passing through the outside slit directly onto the calorimeter are by definition the desired signal. Other photons that are internally reflected are unwanted and contribute to the scattered component of the total measured signal. Since the photons can undergo multiple reflections, the process of calculation is naturally iterative. To further complicate matters, the wall reflection can be

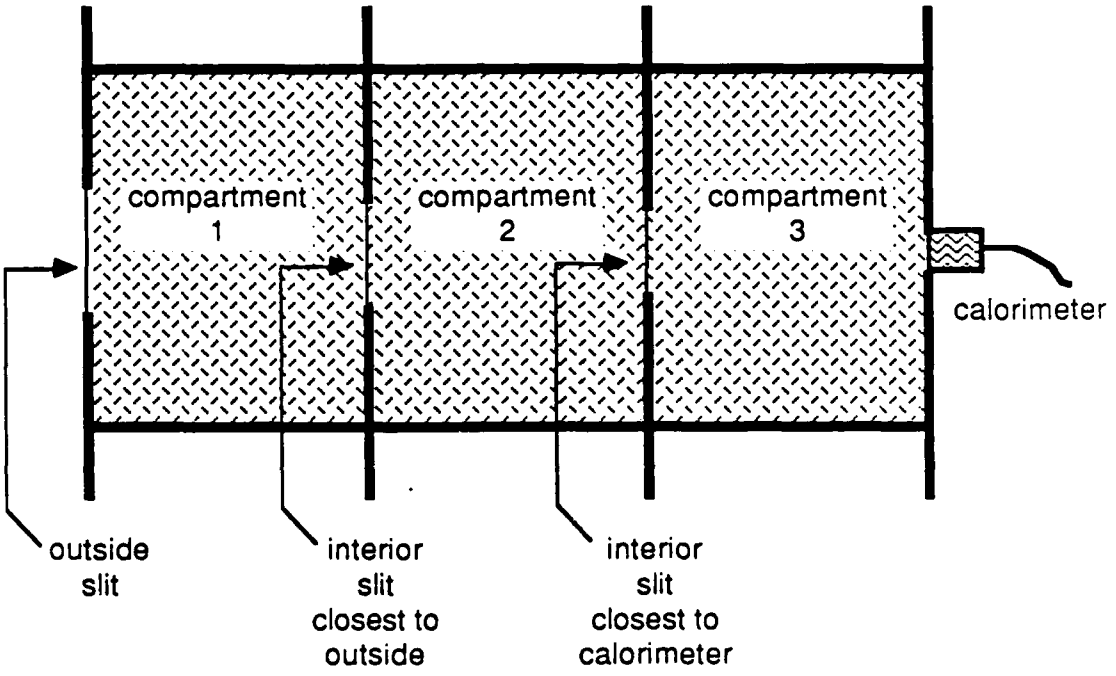

Figure 23. Cross-section of baffled calorimeter.

partially specular and partially diffuse; polarization effects could also be significant.

In order to estimate the effect of the walls and the size of the slits between the compartments on the energy transport, we chose to lump all the effects by computing a probability of photon absorption at a wall to be proportional to the product of the internal surface area within each compartment and its absorptivity. The probability of photons passing through any slit is just its area (i.e., an absorptivity of one). Writing the energy balance results in a set of equations that can be iteratively determined. In order to terminate the iteration a smallness criterion was set.

The entire analysis was performed with the Pascal code shown as Figure 24. One significant advantage of Pascal is its ability to express recursive solutions in an elegant and efficient manner. Procedure INTERACT makes use of this feature and is the essence of the solution technique.

5.4 RESULTS OF INTERNAL SCATTERING ANALYSIS.

Figure 25 and Table 4 show what effect different baffle configurations could have on the measured value when compared to what should be measured if there were no internal scattering within the baffle. This ratio the author chose to call gain; its denominator was determined by calculating, with the TRS predictor model algorithms, what would be directly incident upon the calorimeter with an optical stop equal to the baffle's first slit (the entrance). Its numerator was determined by calculating, also with the TRS predictor model algorithms, what is incident upon the first slit from one flame (it can be also done for the four flames -- the gain would go up slightly for this configuration) and then determining with the N-BAFFLE code

Table 4. Gain from 1 nozzle flame for baffled calorimeter

Height(feet)	2(0.25)A	2(0.25)B	3(0.25)	4(0.25)	2(0.8)	3(0.8)
1	1.480	1.449	1.184	1.052	1.076	1.015
3	1.312	1.292	1.119	1.034	1.049	1.010
5	1.315	1.295	1.121	1.034	1.050	1.010
7	1.336	1.314	1.129	1.037	1.053	1.011
9	1.366	1.343	1.140	1.040	1.056	1.012
11	1.419	1.392	1.160	1.046	1.066	1.013
13	1.600	1.562	1.230	1.065	1.095	1.019

key:	compartments	absorptivity	baffle removed
2(0.25)A	2	0.25	left
2(0.25)B	2	0.25	right
3(0.25)	3	0.25	none
4(0.25)	4	0.25	one added
2(0.8)	2	0.8	right
3(0.8)	3	0.8	none

how much gets scattered into the calorimeter that was not already directly impinging onto it.

```
($S+) (Version: 28 Apr 83)
Program N-Baffle;
USES transcent, ($U*BIG.LIBRARY) mathtrap;
CONST
     version = 'Pascal[1.1]  N-Baffle Code  BSC[2.1];
     reallen = 20;
     max-boxes = 11; (max number of boxes plus one)
     max-try = 5;
TYPE
     direction = (lower, stays, higher);
     (lower and higher box number, or those that stay (i.e., are absorbed)
VAR
     num-boxes: INTEGER;
     cases, pr,baff:TEXT;
     holes: ARRAY [0..max-boxes] OF REAL; (holes into/out of each box)
     wall,alpha,denom: ARRAY [0..max-boxes] OF REAL; (each 0 is a dummy)
     counters: ARRAY [0..max-boxes] OF REAL;
     f: ARRAY [lower..higher,0..max-boxes] OF REAL;
     i,n:INTERGER
     done:BOOLEAN;
     flux-in, flux-cal,
     scat-flux, total: REAL;
     accuracy: REAL;
     small: ARRAY [0..max-boxes] OF REAL;
     ss,s: STRING;
     try: INTEGER;
(-------------------------------------------------------------------------)

PROCEDURE error (msg: STRING);
BEGIN
  PAGE(OUTPUT): GOTOXY(0,11); WRITE(msg);
  CLOSE(pr); CLOSE(cases); CLOSE(baff);
  EXIT(PROGRAM)
END;

(-------------------------------------------------------------------------

PROCEDURE get-arrays;
VAR count: INTEGER; done: BOOLEAN;
BEGIN
  ($1-)
  try:=0;
  REPEAT
    GOTOXY (0,10);
    CLOSE(baff);
    ss :='N-BAFFLES.TEXT';
   WRITELN('File for Baffle Data [default <RETURN>= N-BAFFLES.TEXT] ? ');
    READLN(s);IF LENGTH(s) < = 0 THEN s: = ss;
    RESET(baff,s); (Baffle Data MUST be on PREFIXED VOLUME)
    try : = try + 1;
  UNTIL (IORESULT = 0) OR (try > max-try);
  IF try > max-try THEN error ('Baffle Data File NOT found');
  ($1+)
  count: = 0; done : = FALSE;
```

Figure 24. N-baffle code.

```
WRITE(pr, 'Baffle Data: (hole, wall, alpha) for file: ',s);
WRITELN(pr);
READLN(baff, accuracy);
WRITELN(pr,'Accuracy condition is set to: ',accuracy);
WRITELN(pr);
WHILE (NOT EOF(baff)) AND (count < max-boxes) AND (NOT done) DO
BEGIN
  READLN(baff,holes[count], wall[count], alpha[count]);
  done: = (holes[count] < = 0.0) OR (alpha[count] < 0.0)
                      OR (alpha[count] > 1.0);
  IF NOT done THEN WRITELN(pr,count:5, holes[count]: 15:4,
             wall[count]: 15:4, alpha[count]: 15:4);
  count: = count + 1;
 END;
WRITELN(pr);
CLOSE(baff);
num-boxes: = count - 1; IF num-boxes = 0 THEN EXIT(Program);
END;
(-------------------------------------------------------------------------)
  PROCEDURE fill-arrays;
  VAR n: INTEGER;
  BEGIN
    FOR n: = 1 TO num-boxes DO denom [n]: = holes[n-1]+
                      alpha[n]*wall[n] + holes[n];
    f[higher, o]: = 1.0; f[stays, 0]: = 0.0; f[lower, 0]: =0.0;
    FOR n: = 1 TO num-boxes DO
      BEGIN
       f[lower, n]: = holes[n-1]/denom[n];
       f[stays, n]: = alpha[n]*wall[n]/denom[n];
       f[higher, n]: = holes [n]/denom[n];
    END;
  END;
(-------------------------------------------------------------------------)
PROCEDURE tally (photons: REAL; box: INTEGER);
BEGIN
  GOTOXY (60,2); WRITE('Memory left = ',MEMAVAIL:5);
  GOTOXY (0,4); WRITE(photons:15:5,'photons being added to box',box:2);
  counters[box]: = adder (counters[box],photons);
END;
(-------------------------------------------------------------------------)
PROCEDURE interact (photons: REAL;box: INTEGER);
VAR num-low, num-mid, num-high: REAL;
BEGIN
  IF (box = 0) OR (box = num-boxes + 1) THEN tally (photons, box)
  ELSE
   BEGIN
     num-low :=muler (photons, f[lower, box]);
     IF num-low > small [box-1] THEN interact (num-low, box-1);
     num-high:=muler(photons, f[higher, box]);
     IF num-high > small [box+1] THEN interact (num-high, box+1);
     num-mid :=muler(photons f[stays, box]);
     tally (num-mid,box)
   END;
END;
```

Figure 24. N-baffle code (continued).

```
(------------------------ ----------------------------------------------------)
PROCEDURE write-stuff;
BEGIN
  writeln(pr,'Fractions:  out >->  in <-<-<  stays     at box #');
  writeln(pr,'          --------- --------- ---------          --');
  For i:= 0 to num-boxes Do
   writeln(pr,'':12,
          f[higher,i]:10:5,f[lower,i]:10:5,f[stays,i]:10:5,i:15);
  writeln(pr);
END;
(----------------- ----------------------------------------------------------)
PROCEDURE write-em;
BEGIN
  writeln;
  writeln(pr,'Flux into system     =',flux-in:10:3);
  writeln(pr,'Direct at calorimeter = ',flux-cal:10:3);
  writeln(pr,'Scattered flux       =',scat-flux:10:3);
  writeln(pr,'Total on calorimeter =',total:10:3);
  writeln(pr,'GAIN
              total/flux-cal:10:3);
  writeln(pr);
  writeln(pr); writeln;
END;
(------------------------------------------------------------------------------)
PROCEDURE open-cases;
BEGIN
  {$I-}
  try:=0;
  REPEAT
    GOTOXY (0,15);
    CLOSE(cases);
    ss:='N-B.CASES.TEXT';
    WRITELN('File for Cases [default <RETURN>=N-B.CASES.TEXT] ?');
    READLN(s); IF LENGTH(s) <= 0 THEN s: = ss;
    RESET(cases,s); Data MUST be on PREFIXED VOLUME if default)
    try: = try + 1;
  UNTIL (IORESULT = 0) OR (try >max-try);
  IF try > max-try THEN error ('Cases File NOT found');
  {$I+}
END;
(---------- ---------------------------------------------------------------

BEGIN
  CLOSE(pr);
  REWRITE(pr,'PRINTER:');
  PAGE(pr);
  writeln(pr,version); writeln(pr); writeln(pr);
  get--arrays; (sets num-boxes)
  fill--arrays;
  write--stuff;
  open-cases;
  done: = FALSE;
```

Figure 24. N-baffle code (continued).

```
  WRITELN(pr,'Cases Data: (flux-in, flux-cal) for file:',s);
  WRITELN(pr);
  WHILE(NOT EOF(cases)) AND (NOT done)DO
    BEGIN
      READLN(cases,flux-in, flux-cal);
      done: - (flux-in <=0.0) OR (flux-cal<0.0);
      IF NOT done THEN
        BEGIN
          FOR n: = 0 TO num-boxes + 1 DO counters[n]: = 0;
          (Power absorbed)
          scat-flux: = (flux-in * holes[0]-
               flux-cal*holes[num-boxes]);
          small [0]: = accuracy*scat-flux;
          FOR n: = 1 TO num-boxes + 1 DO (incident upon each box)
            small[n]: = small [n-1]*f[higher, n-1];
          interact (scat-flux,1);
          writeln(pr);
          FOR i: = 0 TO num-boxes + 1 DO
            WRITELN(pr,'Box',i:2,'absorbed',counters[i]:15:5);
          writeln(pr);
          scat-flux: = counters[num-boxes + 1];
          (Scattered flux absorbed by detector)
          scat-flux: = scat-flux/holes[num-boxes];
          total: = flux-cal + scat-flux;
          write-em;
          END;
    END;
  CLOSE(cases);
  CLOSE(pr);
END.
```

Figure 24. N-baffle code (concluded).

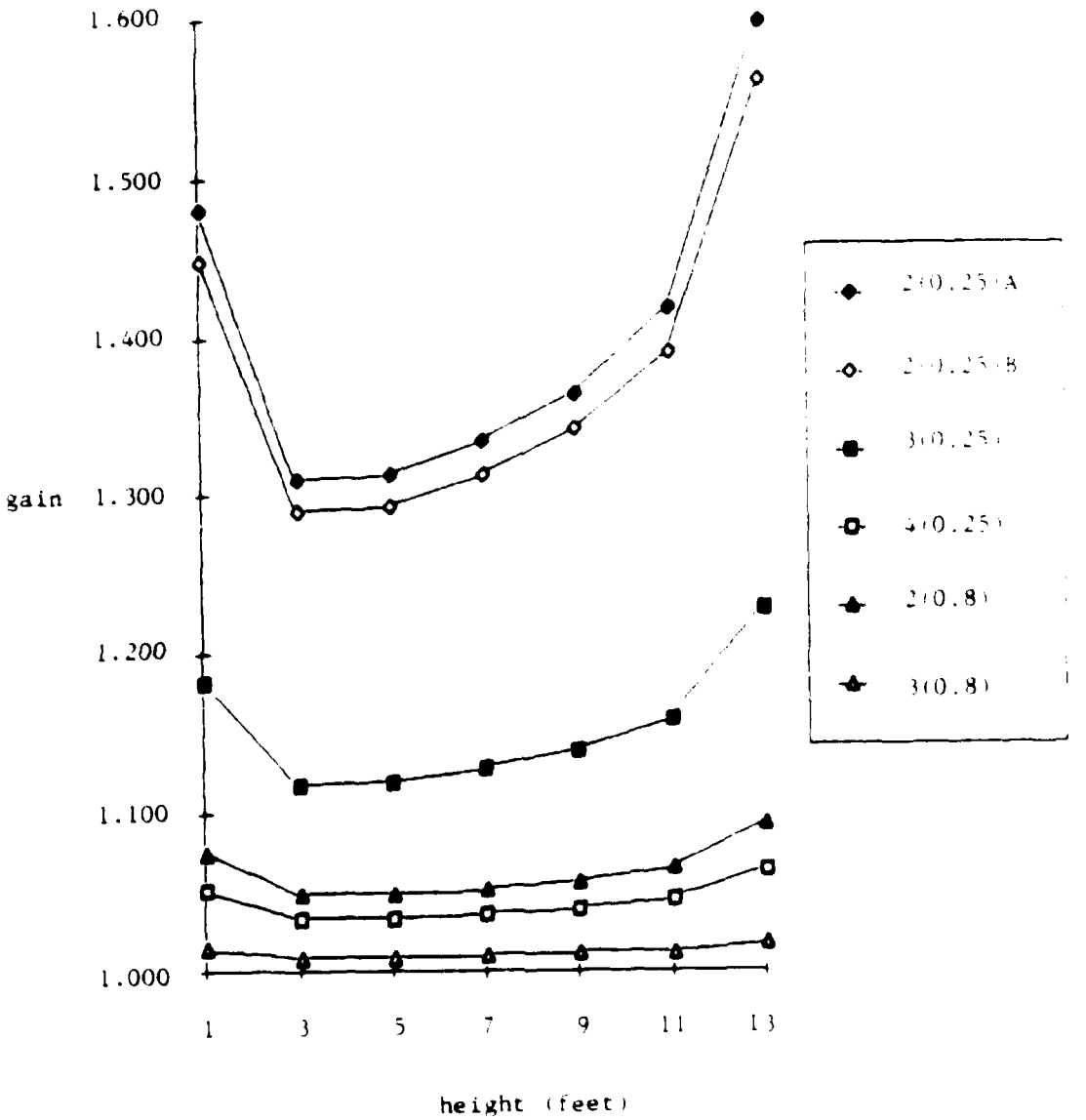

Figure 25. Gain using baffles.

Since the M-BAFFLE code only represents an energy balance approach [illegible] not been validated for its accuracy to this application, it is only used to estimate how many baffles are needed and what internal absorption is required. The application of these results was to be conservative, i.e., more was provided than the analysis indicated so long as costs were not appreciably effected.

In the figure, where one slit is removed the curve is identified as having 2 compartments, where no slit is removed, the curve is identified as having 3 compartments. The curve showing four compartments is for a design with one more compartment which is not shown in Figure 21. For the 2 compartment case where the wall absorptivity is 0.25, the effect of which slit is removed is also shown.

The conclusion drawn was that there should be at least 3 baffle sections (i.e., two internal stops of the type being used) and a blackening of the inside to achieve an absorptivity of the order of 80 percent.

As a result of this analysis, subsequent baffled calorimeter measurements were made with 3 compartments and the interior walls were blackened to increase absorptivity. The first measurement had been made with an untreated galvanized steel interior with only two compartments (i.e., one internal stop). These had clearly been inadequate.

5.5 RESULTS OF MODEL IMPROVEMENT.

The above analysis relied on the model, that we were trying to improve, for estimating the environments inside the baffled calorimeters. Since the measurements were made attention was directed to improving the model.

The results of the baffled calorimeter measurements resulted in changing the model by including an actual flame profile (i.e., rather than a constant height rather than the inverted cone, which was how the flame was modeled prior to this effort. Figure 26 shows the result of the improved model predictions along with the measurements. The new model is in better agreement with the measured height dependency than the earlier model predictions.

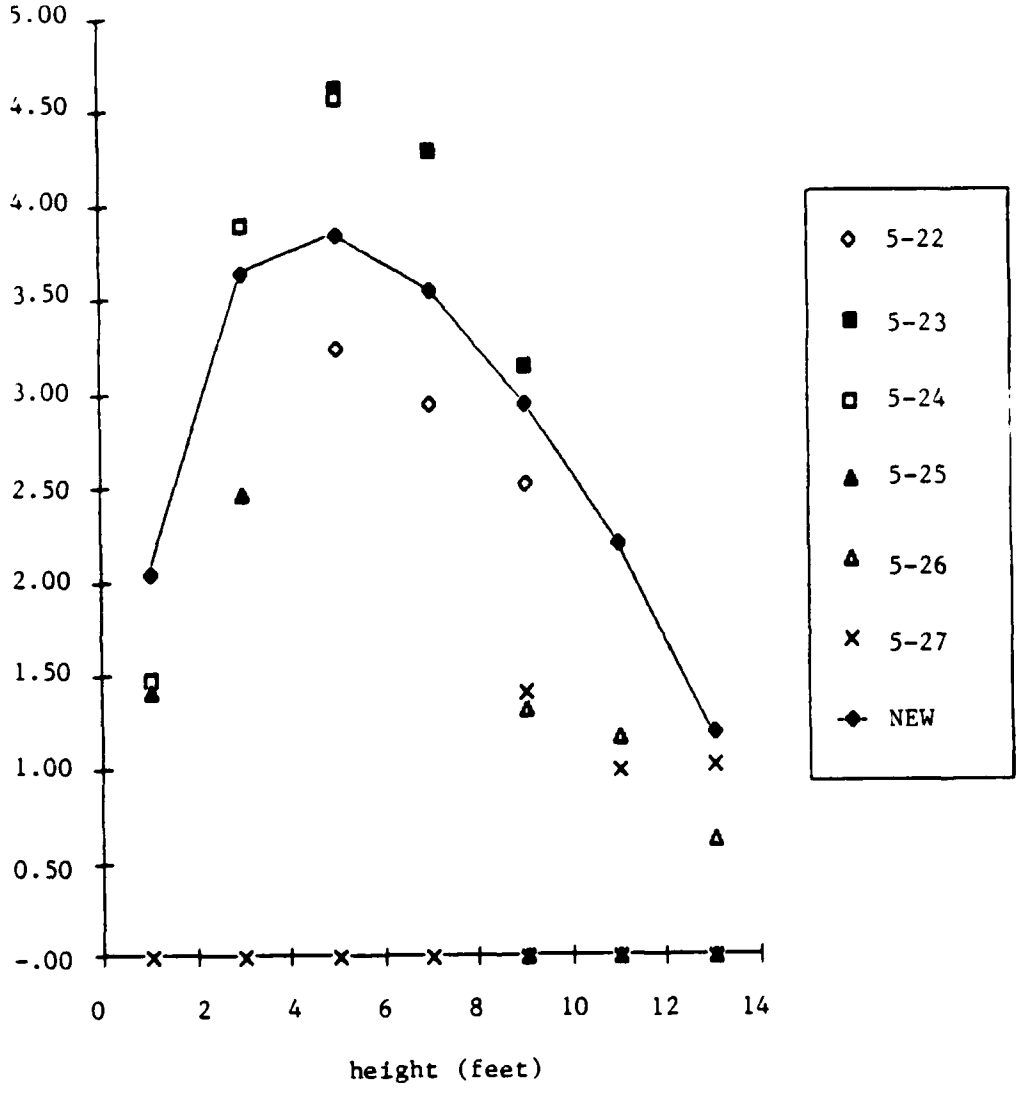

Figure 26. Baffled calorimeter data.

SECTION 6

CONCLUSIONS AND RECOMMENDATIONS

This section presents the conclusions and recommendations that resulted from this effort; these are grouped by topic.

6.1 PLANNED LB/TS TRS FLAME.

The current plan is to include a new type of TRS, called the thin-flame, in the LB/TS. The intent is to produce a flame that is smaller in range extent so that it can be vented easier and hopefully allow objects to be set closer to it and thereby possibly increase the irradiance. The flame would fan out in cross range. Therefore, the results obtained here, while helpful to modeling TRS environments may have to be extended to this new TRS. It is also possible that only a calibration of the current TRS model will be required to replicate the thin-flame TRS data. Until data are available, it will remain unclear as to which path should be taken.

6.2 SCALING TO FUEL FLOW RATE.

While the scaling of TRS output to fuel flow rate is inconclusive, the trends that have been inferred will warrant further inspection when more data become available. In order to preserve what has been done, but at the risk of the reader taking the following comments to mean that the scaling relationships have been established, it is hypothesized that the power out parameter will scale directly with the fuel flow rate for certain similar TRS operational parameters. Further, it is hypothesized that the volume of the flame scales directly with the square root of the fuel flow rate ratio. Both of these hypotheses are very preliminary and based on too few data. Nevertheless, since it is conceivable that such hypotheses may facilitate comparison of future data they have been included.

6.3 PHOTOGRAPHIC AND SPECTRAL MEASUREMENTS.

An attempt to model the photographic and spectral measurement results should be made.

Measurements in the infrared should be considered and possibly made in order to determine the nature of the flame's radiance and these compared to the optical data. A dual wavelength (3 to 5 and 8 to 12 microns) observation of the TRS could be helpful. It would be beneficial to include a larger fraction of the spectrum than just the visible because the TRS spectrum is apparently less than 3000 degrees Kelvin.

6.4 BAFFLED CALORIMETER MEASUREMENTS.

It is recommended that baffled calorimeter data be reacquired on a dedicated set of TRS burns and a larger number of calorimeters be used. DNA Field Command now has at least thirty calorimeters for use at the TRS site; the TRS flux field can now be measured in greater detail.

Additional measurements with the limited field of view calorimeters would be beneficial if a few non-windy tests could be performed with at least six of these gauges on the same pole. The baffle units could also be improved

somewhat to further reduce internal scattering.

6.5 CALORIMETER RESPONSE.

Most of the prior data from TRS burns have been acquired with fielded calorimeters. These calorimeters were supplied by the manufacturer with calibration curves providing generated sensor voltage as a function of delivered thermal flux. The source used to generate the calibration curves has not been identified and the spectral sensitivity of the calorimeter front surface is unknown. Additionally, to use the calorimeter data, it has been assumed that the sensors have on ideal isotropic response to delivered flux. This has not been validated, and in general calorimeter response has not been characterized with as much detail as is necessary for efficient model development and validation. It is recommended that this information be obtained.

6.6 SPOT CHECK OF CALORIMETER RESPONSE.

One additional item of note is the fact that there is currently no way to assess calorimeter response just prior to a shot. A readiness condition is tested by briefly exposing each calorimeter to the flame of a portable propane torch. Response is noted but not quantized. Again, to assure a common base to the data, and that certain biases have not been introduced, spot checks should be developed for the LB/TS and also the field.

SECTION 7

LIST OF REFERENCES

1. Kitchens, C. W. Jr., Lottero, R. E., Mark A.. and Teel, G. D., "Blast Wave Modifications during Combined Thermal Blast Simulation Testing", ARBRL-TR-02352, U.S. Army Ballistics Research Laboratory Technical Report, Aberdeen Proving Ground, MD, July 1981.

2. Chambers, B., "Estimating Radiated Thermal Environments from Aluminum-LOX Thermal Radiation Simulators", Science and Engineering Associates Inc., DNA TR 85-3, December 1984.

3. Chambers, B., "TRS Environment Calculations for event DIRECT COURSE", Science & Engineering Associates, Inc., DNA TR 85-3, June 1985.

4. Rehmann, W., "Characterization of the thermal radiation field generated by a one-nozzle torch", ARBRL-TR-02529, U.S. Army Ballistics Research Laboratory Technical Report, Aberdeen Proving Ground, MD, October 1983.

5. Thompson, F. O., Jr. and Sachs, D.C., "Preliminary Review of LOX-TRS Test Data", Kaman Tempo, 23 February 1983.

6. Teel, G., private communication, 19 April 1983.

7. Teel, G., private communication, 3 April 1984.

8. Chambers, B., "Implementation of Thermal Models and Algorithms of Field Command DNA", Science & Engineering Associates, Inc., DNA TR 85-4, December 1983.

9. Chambers, B., "FC-TEE Version II TRS Environment Predictor", Science & Engineering Associates, Inc., SEA Report No. 104-01-Q:01, July 1985.

10. Teel, G., private communication.

11. Dishon, J., private communication.

12. Dudziak, W., "Radiative Properties of TRS 5-19", Information Sciences, Inc., ISI Report No. RM83-ISI102, July 1983.

DISTRIBUTION LIST

DEPARTMENT OF DEFENSE

ASST TO THE SECY OF DEFENSE ATOMIC ENERGY
ATTN: EXECUTIVE ASSISTANT

DEF RSCH & ENGRG
ATTN: STRAT & SPACE SYS(OS)

DEFENSE INTELLIGENCE AGENCY
ATTN: RTS-2A (TECH LIB)
ATTN: RTS-2B

DEFENSE NUCLEAR AGENCY
ATTN: SPTD
ATTN: STSP
4 CYS ATTN: STTI-CA

DEFENSE TECHNICAL INFORMATION CENTER
12 CYS ATTN: DD

FIELD COMMAND DEFENSE NUCLEAR AGENCY
ATTN: FCT
ATTN: FCTT
ATTN: FCTXE

JOINT CHIEFS OF STAFF
ATTN: GD50 J-5 FOR PLNG & PROG DIV
ATTN: J-5 NUCLEAR DIV/STRATEGY DIV
ATTN: JAD

DEPARTMENT OF THE ARMY

HARRY DIAMOND LABORATORIES
2 CYS ATTN: SCHLD-NW-P
ATTN: SCLHD-DTSO (00103)
ATTN: SLCHD-NW-RA L BELLIVEAU
ATTN: SLCIS-IM-TL (81100) (TECH LIB)

U S ARMY ATMOSPHERIC SCIENCES LAB
ATTN: SLCAS-AE

U S ARMY BALLISTIC RESEARCH LAB
ATTN: SLCBR-SS-T (TECH LIB)
ATTN: SLCBR-TB-B R RALEY
2 CYS ATTN: SLCBR-TB-D A PEARSON
ATTN: SLCBR-TB-R A MARK

U S ARMY CORPS OF ENGINEERS
ATTN: DAEN-RDL

U S ARMY ENGR WATERWAYS EXPER STATION
ATTN: D OUTLAW
ATTN: TECHNICAL LIBRARY
ATTN: WESSE

U S ARMY FOREIGN SCIENCE & TECH CTR
ATTN: DRXST-SD

U S ARMY MATERIAL COMMAND
ATTN: AMCCN
ATTN: DRXAM-TL (TECH LIB)

U S ARMY NUCLEAR & CHEMICAL AGENCY
ATTN: LIBRARY
ATTN: MONA-NU

U S ARMY TEST AND EVALUATION CMD
ATTN: DRSTE-CM-F R GALASSAO

U S ARMY TRADOC SYS ANALYSIS ACTVY
ATTN: ATAA-TDC R BENSON

US ARMY WHITE SANDS MISSILE RANGE
ATTN: STEWS-DE-DT R HAYS
ATTN: STEWS-FE-R
ATTN: STEWS-TE-N K CUMMINGS
ATTN: STEWS-TE-N T ARELLANES

DEPARTMENT OF THE NAVY

NAVAL RESEARCH LABORATORY
ATTN: CODE 2627 (TECH LIB)
ATTN: CODE 4700 W ALI
ATTN: CODE 4720 J DAVIS
ATTN: CODE 5584 E FRIEBELE
ATTN: CODE 6584 G SIGEL
ATTN: CODE 7780

NAVAL SURFACE WEAPONS CENTER
ATTN: CODE H14
ATTN: CODE X211 (TECH LIB)

NAVAL SURFACE WEAPONS CENTER
ATTN: TECH LIBRARY & INFO SVCS BR

STRATEGIC SYSTEMS PROGRAM OFFICE (PM-1)
ATTN: NSP-L63 (TECH LIB)

DEPARTMENT OF THE AIR FORCE

AERONAUTICAL SYSTEMS DIVISION
ATTN: ASD/ENSS

AIR FORCE INSTITUTE OF TECHNOLOGY/EN
ATTN: LIBRARY/AFIT/LDEE

DEPARTMENT OF THE AIR FORCE (CONTINUED)

AIR FORCE WEAPONS LABORATORY, AFSC
ATTN: NTE M PLAMONDON
ATTN: NTED R HENNY
ATTN: NTES-G
ATTN: SUL

OTHER GOVERNMENT

CENTRAL INTELLIGENCE AGENCY
ATTN: OSWR/NED

DEPARTMENT OF COMMERCE
ATTN: SEC OFC FOR R LEVINE

DEPARTMENT OF DEFENSE CONTRACTORS

DAYTON, UNIVERSITY OF
ATTN: B WILT
ATTN: D GERDEMAN
ATTN: N OLSON
ATTN: R SERVAIS

KAMAN SCIENCES CORP
ATTN: LIBRARY

KAMAN SCIENCES CORP
ATTN: E CONRAD

KAMAN TEMPO
ATTN: DASIAC
ATTN: W CHAN

KAMAN TEMPO
ATTN: DASIAC

NICHOLS RESEARCH CORP, INC
ATTN: R BYRN

PACIFIC-SIERRA RESEARCH CORP
ATTN: H BRODE, CHAIRMAN SAGE

R & D ASSOCIATES
ATTN: F A FIELD
ATTN: P RAUSCH
ATTN: TECHNICAL INFORMATION CENTER

SCIENCE & ENGRG ASSOC INC
2 CYS ATTN: J STOCKTON

SCIENCE & ENGRG ASSOC.,INC
2 CYS ATTN: B CHAMBERS

SCIENCE APPLICATIONS INTL CORP
ATTN: J DISHON

SCIENCE APPLICATIONS INTL CORP
ATTN: TECHNICAL LIBRARY

SCIENCE APPLICATIONS INTL CORP
ATTN: J MCRARY

SCIENCE APPLICATIONS INTL CORP
ATTN: TECHNICAL LIBRARY

SCIENCE APPLICATIONS INTL CORP
ATTN: J COCKAYNE
ATTN: R SIEVERS
ATTN: W CHADSEY
ATTN: W LAYSON

FOREIGN

ATOMIC WEAPONS RESEARCH ESTABLISHMENT
ATTN: D SAMUELS

BRITISH DEFENCE STAFF
ATTN: ACOW

CENTRE D'ETUDES, GRAMAT
ATTN: J MALAVERGNE

DRET
ATTN: F ISTIN

ERNST-MACH INSTITUT
ATTN: H REICHENBACH

END

3-87

DTIC